

Holographic quantum criticality and strange metal transport

Bom Soo Kim^a, Elias Kiritsis^{b,c} and Christos Panagopoulos^{b,d,e}

^a Raymond and Beverly Sackler School of Physics and Astronomy,
Tel Aviv University, 69978 Tel Aviv, Israel;

^b Crete Center for Theoretical Physics, Department of Physics,
University of Crete, 71003 Heraklion, Greece;

^c APC, AstroParticule et Cosmologie, Université Paris Diderot, CNRS/IN2P3,
CEA/IRFU, Observatoire de Paris, Sorbonne Paris Cité,
10, rue Alice Domon et Léonie Duquet, 75205 Paris Cedex 13, France

^d IESL-FORTH, 71110 Heraklion, Greece;

^e Division of Physics and Applied Physics,
Nanyang Technological University, 637371 Singapore

Abstract

A holographic model of a quantum critical theory at a finite but low temperature, and finite density is studied. The model exhibits non-relativistic $z=2$ Schrödinger symmetry and is realized by the Anti-de-Sitter-Schwarzschild black hole in light-cone coordinates. Our approach addresses the electrical conductivities in the presence or absence of an applied magnetic field and contains a control parameter that can be associated to quantum tuning via charge carrier doping or an external field in correlated electron systems. The Ohmic resistivity, the inverse Hall angle, the Hall coefficient and the magnetoresistance are shown to be in good agreement with experimental results of strange metals at very low temperature. The holographic model also predicts new scaling relations in the presence of a magnetic field.

Contents

1	Introduction	3
2	Holography and AdS/CFT for strongly correlated electrons	5
3	Schrödinger geometry	8
3.1	Schrödinger geometry and its interpretation	9
3.2	The role and interpretation of the parameter b	10
4	Holographic DBI transport	11
4.1	Strong-coupling transport mechanisms	13
4.2	The role and interpretation of the parameter E_b	14
5	Holographic Hall transport	16
6	Comparison to experiment	17
6.1	Resistivity	19
6.2	Inverse Hall angle	20
6.3	Magnetoresistance	21
6.4	Hall coefficient	22
6.5	Köhler rule	23
7	Outlook	23
	Acknowledgments	24
	APPENDIX	25
A	Detailed calculation of the conductivity	25
A.1	Conductivity calculation with E_b^y and E_b^z	25
A.2	Hall conductivity calculation	27

B	Study of the temperature dependence of the conductivity.	29
B.1	Drag dominated regime	29
B.1.1	Drag dominated regime I : $\mathcal{B} \ll t^2$	31
B.1.2	Drag dominated regime II : $\mathcal{B} \gg t^2$	31
B.2	Pair creation dominated regime	32
B.2.1	Pair creation dominated regime I : $\mathcal{B} \ll t^2$	32
B.2.2	Pair creation dominated regime II : $\mathcal{B} \gg t^2$	33
B.2.3	Condition for the drag dominated regime	33

1 Introduction

Strongly correlated electron systems have challenged traditional condensed matter paradigms with weakly interacting quasiparticles [1]. Meanwhile, theory tools originating from high-energy physics have been useful in addressing the physical properties of these materials, (for a review see [2]). For example, the anti de-Sitter / Conformal Field Theory (AdS/CFT) correspondence has proved successful in the investigation of strong-coupling gauge theories [3] with its first application focusing on conformally invariant theories.

Other non-relativistic scaling symmetries have been proposed in the context of holography involving Schrödinger symmetry [4, 5] or Lifshitz symmetry [6]. The progress in geometric realizations of Schrödinger symmetry, with a general dynamical exponent z , aimed for condensed matter applications has paved the way to finite temperature generalizations [7, 8, 9, 10] using the null Melvin twist [11, 12].

AdS space in the light-cone frame (ALCF) with $z=2$, has also been put forward [13, 14], as such a holographic background and a corresponding Schwarzschild black hole solution have been considered [8, 15]. Notably, while Schrödinger space and ALCF yield the same thermodynamic properties [7, 8, 10, 15] and transport coefficients (when the latter are independent of an embedding scalar) [16, 15], ALCF is simpler and has a well-defined holographic renormalization.

Here we will analyze and report on the transport properties of ALCF, matching several universal experimental results of the normal-state of cuprates superconductors at very low temperatures, which have been a subject of intensive research and yet remain largely unexplained over the past two decades. While there are other types experimental data available, such as spectroscopy and thermodynamic data, we choose to analyze transport data because

an understanding of the normal state transport properties of high T_c cuprates is widely regarded as a key step towards the elucidation of the pairing mechanism for high-temperature superconductivity [17].

The holographic model we present provides a novel paradigm for the normal state of strange metals, in particular high-temperature superconducting (high T_c) cuprates in the overdoped region, where the charge carriers added to the parent insulator exceed the value necessary for optimal superconductivity. Further to describing the puzzling normal state properties of these materials, our approach leads to new falsifiable predictions for experiment. In particular, we successfully describe the $T + T^2$ behavior of the resistivity in [18] and the $T + T^2$ behavior of the inverse Hall angle observed in [19] at *very low temperatures* $T < 30K$, where a single scattering rate is present.

This newly emerging very low temperature scaling behaviors of magnetotransport properties are in accord with the distinct origin of the criticality at very low temperatures advertised in [20], while the higher temperature, $T > 100K$, scaling has different behaviors between the linear temperature resistivity and the quadratic temperature inverse Hall angle, signaling two scattering rates [21]. In searching for quantum criticality at zero temperature and its possible connection to the origin of superconductivity, we concentrate on the lower temperature regime with a single scattering process. We also comment on how two scattering processes emerge by incorporating other mechanisms present in our model.

In addition to the resistivity and inverse Hall angle, very good agreement is also found with experimental results of the Hall Coefficient, magnetoresistance and Köhler rule on various high T_c cuprates [18, 19, 20, 21, 22, 23, 24, 25, 26, 27, 28, 29, 30, 31, 32, 33, 34]. To the best of our knowledge, no other model that describes all of these observables successfully. Our model provides a change of paradigm from the notion of a quantum critical point, as it is quantum critical at $T \rightarrow 0$ on the entire overdoped region. In this sense our work breaks apart from other holographic approaches [35, 36, 37], where the measured transport is due to loop fermion effects. As such, it is applicable to a more general class of materials *e.g.*, d and f -electron systems, where the low temperature resistivity varies as $T + T^2$ [38] and exhibit a quantum critical line [18, 39].

There have been several works that use holographic approaches in order to model strange metal behavior. The fermionic structure of such systems in the IR has been analyzed in [35, 36, 37] and modifications due to dipole couplings in [40]. In particular, it was found that there is an IR scaling symmetry that could allow the realization of a marginal Fermi liquid. The IR exponent would need, however, to be tuned for this to take place.

The linear temperature dependence of the Ohmic resistivity was realized in spaces with

AdS or Lifshitz scaling [41, 42, 43, 44] and in Schrödinger space [16, 15]. A linear resistivity and a crossover to quadratic behavior was found in a larger class of scaling geometries in [43]. In the same reference, the full set of possible holographic non-trivial low temperature behavior was classified and, as shown in [45], comprises all possible classes of quantum critical behavior in theories with a single scalar IR relevant operator dominating the dynamics. Finally, the temperature behavior of the Hall angle was addressed using Lifshitz type metric with broken rotational symmetry [46].

In section 3, we provide the basic information for the gravity background, including how to interpret the background compared to the extensively studied AdS. Then, we provide detailed properties and calculations of the transport data using the probe DBI technique in section 4. Magnetotransport coefficients are calculated and analyzed in section 5, where we also include the analysis of higher-temperature transport properties. Our data is compared to the experimental results available in the literature, focusing on the universal features in section 6.

2 Holography and AdS/CFT for strongly correlated electrons

Strong interactions of realistic finite-density systems have provided an arena for a wealth of techniques, geared to assess in most cases the qualitative physics. A wide range of unsolved problems remain to be addressed, especially in the realm of strange metals including condensed matter systems on the border with magnetism. There is, therefore, an inviting opportunity for new techniques and approaches to contribute in these challenging problems in modern condensed matter. An interdisciplinary approach towards this aim is the utilization of the gauge-gravity correspondence, abstracted from the correspondence between non-abelian gauge theories and string theories. So far it has been explored in several directions, providing a novel perspective both in the modelization as well as solution of some strongly coupled QFTs. The hope behind potential applications to condensed matter physics is that IR strong interactions of the Kondo type in materials, where spins can interact with electrons, may provide bound states that behave in a range of energies as non-abelian gauge degrees of freedom that may also be coupled to other fields. The gauge interactions are characterized by a number of charges N_c that are conventionally called “colors”. Their actual number depends on the problem at hand but it is typically small.

If this is the case, then in terms of the electrons and spins, the YM fields are composite. In the regime where the effective YM interaction is strong, the physical degrees of freedom

are expected to be colorless bound states. Their residual interactions, analogous to nuclear forces in high-energy physics, are still strong. On the other hand, the effective interaction between colorless bound states can be made arbitrarily weak in the limit of a large number of colors, $N_c \rightarrow \infty$, as it is controlled by $1/N_c \rightarrow 0$, although the original interaction of colored sources is strong. In this limit, the theory is simplified and may be calculable. Of course, typically, the original problem has a finite and sometimes small number of effective colors. The question then is: how reliable are the large N_c estimates for the real physics of the system? The answer to this varies, and we know many examples in both classes of answers. A good example on one side is the fundamental theory of strong interactions, Quantum Chromodynamics based on the gauge group $SU(3)$, indicating $N_c = 3$ colors. It is by now established that for many aspects of this theory, $3 \simeq \infty$, the accuracy varies in the range 3 – 10%. It is also known that the analogous theory with two colors, $SU(2)$, has some significant differences from its $N_c \geq 3$ counterparts. There are other theories where the behavior at finite N_c is separated from the $1/N_c$ expansion by phase transitions making large N_c techniques essentially inapplicable.

Notably, large N_c techniques have been applied to strongly coupled systems for several decades, and it is therefore natural to ask for the new contribution delivered in the present effort. In adjoint theories in more than two dimensions, it is well known that until recently even the leading order in $1/N_c$ could not be computed. Although some qualitative statements could be made in this limit, the number of quantitative results was rather scarce. On the other hand, 't Hooft observed that the leading order in $1/N_c$ is captured by the classical limit of a quantum string theory [47]. Finding and solving this classical string theory was therefore equivalent to calculating the leading order result in $1/N_c$ in the gauge theory. Unfortunately, such string theories, dual to gauge theories, remained elusive until 1997, when Maldacena [48] made a rather radical proposal: (a) This string theory lives in more dimensions than the gauge theory¹; (b) At strong coupling, it can be approximated by supergravity, a tractable problem. The concrete example proposed contained on one hand a very symmetric, scale invariant, four-dimensional gauge theory (N=4 super Yang-Mills), and on the other a ten-dimensional IIB string theory compactified on the highly symmetric constant curvature space $AdS_5 \times S^5$. Therefore, this correspondence becomes to be known as the AdS/CFT, or holographic, correspondence.

Although this claim is a conjecture, it has amassed sufficient evidence to spark consider-

¹This unexpected (see however [49]) fact can be intuitively understood in analogy with simpler adjoint theories in 0 or 1 dimensions. There it turns out that the eigenvalues of the adjoint matrix in the relevant saddle point become continuous in the large N_c limit, and appear as an extra dimension. In general how many new dimensions may emerge in a given QFT in the large N_c limit is not a straightforward question to answer, although exceptions exist.

able theoretical work exploring the ramifications of the correspondence, for the dynamics on one hand of strongly coupled gauge theories and on the other hand of strongly curved string theories.

An important evolution of the holographic correspondence is the advent of the concept of Effective Holographic Theories (EHTs) [43] in analogy with the analogous concept of Effective Field Theories (EFTs) in the context of QFT². The rules more or less follow those of EFTs with some obvious differences and most importantly with less intuition.

In standard EFTs, there are several issues that are relevant: (a) Derivation of the low energy EFT from a higher energy theory; (b) Parametrization of the interactions of an EFT, and their ordering in terms of IR relevance; (c) Physical Constraints that an EFT must satisfy. Although the Wilsonian approach has allowed a good understanding of EFTs, there are still general questions which can not be answered with our tools, for instance whether a given EFT can arise as the IR limit of a UV complete QFT.

In the context of holographically dual string theories, many issues are still not fully understood. First and foremost is that the classical string theories dual to gauge theories cannot yet be solved. The only approximation making these tractable is the (bulk³) derivative expansion. This reflects the effect of the string oscillations on the dynamics of the low-lying string modes.

It is known in many cases and widely expected that such an expansion is controlled by the strength of the QFT interactions. In the limit of infinite strength, the string becomes stiff and the effects of string modes may be completely neglected. The theory then collapses to a gravitational theory coupled to a finite set of fields. Since we are working to leading order in $1/N_c$, the treatment of this theory is purely classical. Observables (typically boundary observables corresponding to correlators of the dual CFT) are computed by solving second-order non-linear differential equations.

The effects of finite but large coupling are then captured by adding higher-derivative interactions in the gravitational action. Note that this derivative expansion is not directly related to the IR expansion of the dual QFT.

The bulk theory, as mentioned earlier, has usually more dimensions compared to those of the dual QFT. One of them is however special: it is known as the “holographic” or “radial” dimension, and controls the approach to the boundary of the bulk spacetime. Moreover, it

² There are several works that contain a version or elements of the idea of the EHT [50], although they vary in the focus or philosophy.

³We refer to as the “bulk”, the spacetime in which strings propagate. This is always a spacetime with a single boundary. The boundary is isomorphic to the space on which the dual quantum field theory (gauge theory) lives.

can be interpreted as an “energy” or renormalization scale in the dual QFT.

The second order equations of motion of the bulk gravitational theory, viewed as evolution equations in the radial direction, can be thought of as Wilsonian RG evolution equations [51]. The boundary of the bulk spacetime corresponds to the UV limit of the QFT. Although the equations are second order they need only one boundary condition in order to be solved, as the second condition is supplied by the “regularity” requirement of the solution at the interior of spacetime. Here gravitational physics proves particularly helpful: a gravitational evolution equation with arbitrary boundary data leads to a singularity. Demanding regular solutions gives a unique or a small number of options. The notion of “regularity” can however vary, and may include runaway behavior as in the case of holographic open string tachyon condensation relevant for chiral symmetry breaking [52].

The holographic model and associated saddle point we will explore here is rather simple and does not require a very sophisticated machinery. It has, however, a non-relativistic Schrödinger symmetry, and this is a realm that has not been explored fully so far.

3 Schrödinger geometry

The model we present is comprised of two sectors. The first is gravitational and contains the metric as a single field. It controls the dynamics of energy in the theory, and we will analyze it in this section. The second contains the dynamics of the charge carriers and will be given by a Dirac-Born-Infeld (DBI) action of a gauge field dual to the conserved current of the carriers. We will analyze this part in a later section where we will calculate the conductivities.

The gravitational action is the Einstein action with a negative cosmological constant

$$I = \frac{1}{16\pi G_5} \int d^5x \sqrt{-g} \left(\mathcal{R} + \frac{12}{\ell^2} \right), \quad (1)$$

where the symbols g , \mathcal{R} and ℓ are the determinant of the metric, the scalar curvature and the length scale of the theory related to the cosmological constant, respectively. We suppress the boundary terms needed for proper boundary conditions and renormalization, and consider the AdS-Schwarzschild black hole solution in light-cone coordinates [8, 15]

$$ds^2 = g_{++}dx^{+2} + 2g_{+-}dx^+dx^- + g_{--}dx^{-2} + g_{yy}dy^2 + g_{zz}dz^2 + g_{rr}dr^2, \quad (2)$$

where

$$g_{++} = \frac{(1-h)r^2}{4b^2\ell^2}, \quad g_{+-} = -\frac{(1+h)r^2}{2\ell^2}, \quad g_{--} = \frac{(1-h)b^2r^2}{\ell^2}, \quad g_{yy} = g_{zz} = \frac{r^2}{\ell^2},$$

$$g_{rr} = \frac{\ell^2}{hr^2}, \quad h = 1 - \frac{r_H^4}{r^4}, \quad x^+ = b(t+x), \quad x^- = \frac{1}{2b}(t-x). \quad (3)$$

To ensure $z=2$, we assign $[b]$ (the scaling dimension of b in the unit of mass) as -1 , and thus $[x^+] = -2$ and $[x^-] = 0$. The full 10-dimensional space, $\text{AdS}_5 \times S^5$, in light-cone coordinate was written in *e.g.*, [16][15]. We drop the S^5 part for the rest of our discussion, except for the embedding scalar discussed below, because it is decoupled and becomes an overall factor in the probe brane DBI action [53].

To match the non-relativistic isometry group, one of the light-cone directions, x^+ with scaling dimension -2 , is identified as time, and we fix the momentum of the other light-cone coordinate, x^- [4, 14]. The thermodynamic properties of the ALCF are identical to those of Schrödinger space [7, 8, 10, 15], explained below in section 3.2. The interpretation of this coordinate system is connected to being on the infinite momentum frame along a single spatial direction, which we take here as x . In this frame, the nontrivial physics occurs in the two transverse spatial dimensions y, z .

3.1 Schrödinger geometry and its interpretation

The initial geometry is the AdS Schwarzschild black hole, which is known to describe a strongly coupled Conformal Field Theory (CFT) at finite temperature. However, here it is described in the light-cone coordinate system and since x^+ will be taken as time, the symmetry is broken to a $z=2$ Schrödinger symmetry. In this sense, the bulk background, equations (1)-(3), describe the strongly coupled "glue" that interpolates between conformal symmetry at high temperatures and $z=2$ Lifshitz like non-relativistic scaling symmetry near $T = 0$.

A qualitative way to understand this is to appreciate that in these coordinates the "speed of propagation" of signals in the bulk spacetime asymptotes to zero as we approach the black-hole horizon. This is a well known effect in black hole space-times [54] in this coordinate system - also known as the Carolean limit.

This transition, from AdS critical ($z=1$) to Lifshitz critical ($z=2$), is a key ingredient of the gravitational black hole background. It is important to identify where the transition occurs. In the bulk background, this is controlled by the parameter b . Here, b is a length scale that parametrized precisely this transition, in a way that preserves scale covariance. In brief, the bulk geometry is an interpolation between ($z=1$) and ($z=2$) geometries in the

IR. The associated dual theory should likewise interpolate between two energy regimes, one where it has the usual relativistic scale symmetry and another where it has the Lifshitz symmetry.

It should be noted that the gravitational background is 5 dimensional. Apart from the holographic directions, there is a time direction and 3 regular space directions x, y, z . In light cone coordinates, $x^\pm = x \pm t$, one of the spatial coordinates, namely x , is playing a special role. The Schrödinger frame can be considered as an infinite boost in the x directions (this is the infinite momentum frame in QFT) as we discuss below. In this limit, all dependence on x spacial direction is redundant, hence the physics depends only on two spatial directions y, z . Therefore, it is these two spacial directions that the theory depends upon, and the dual quantum field theory is 2+1 dimensional.

3.2 The role and interpretation of the parameter b

There are two control parameters in this model, b and E_b , which will be introduced in the following section. Both are dimensionful but can form dimensionless combinations either alone or combined with temperature.

The significance of the parameter b can be appreciated physically from the thermodynamics of the same system described in [8][15]. These are as follows:

$$E = \frac{\pi^3 \ell^3 b^4 T^4 V_3}{16 G_5}, \quad J = -\frac{\pi^3 \ell^3 b^6 T^4 V_3}{4 G_5}, \quad S = \frac{\pi^3 \ell^3 b^4 T^3 V_3}{4 G_5}, \quad \Omega_H = \frac{1}{2b^2}, \quad (4)$$

where we have defined $V_3 := \int dx^- dy dz$ and used $r_H = \pi \ell^2 b T$. ℓ is the AdS length, while G_5 is the five-dimensional Newton's constant. J is the charge associated with the translational symmetry in x^- , that is conserved in the Schrödinger geometry, while Ω_H is the associated chemical potential.

To understand the non-relativistic $z=2$ scaling, the mass dimensions of various parameters are $[b] = -1$, $[x^+] = -2$, $[x^-] = 0$, $[y] = [z] = -1$ and $[V_3] = -2$. From $[G_5] = -3$, we obtain $[J] = 0$, $[\Omega_H] = 2$, $[M] = 2$, $[S] = 0$, $[\beta] = -2$ and $[T] = 2$. These are consistent with the dimensions of the non-relativistic systems with the dynamical exponent $z=2$, as described in appendix F in [8].

Therefore, the parameter b can be associated with the chemical potential for the conserved particle number of the Schrödinger symmetry. The dimensionless quantity $b^2 T$ is associated with the crossover behavior between the $z=1$ and $z=2$ regimes of the black hole solutions.

It can be seen from (4) that b controls also the system's response to external pressure. Therefore, different values of b correspond to different external pressures for the “glue” en-

semble. External pressure is a widely used quantum tuning parameter to study the evolution of the ground state electronic properties in a range of strange metals including organic superconductors, heavy fermion systems and other strongly correlated electron systems.

4 Holographic DBI transport

We will now add to the system, charge carriers, using D-branes. To calculate the transport properties, we follow the standard DBI probe approach [55][16][15]. We introduce N_f D7 branes on the background and work in the probe limit, $N_f \ll N_c$. The D7 branes cover three angular directions S^3 of S^5 in addition to the background (eq. (2)). From this embedding there are two remaining world volume scalars on the branes. One scalar is chosen to be trivially constant and the other a function of the radial coordinate $\theta(r)$. Hence, D7 has the same metric as eq. (2) with a simple modification $g_{rr} \rightarrow g_{rr}^{D7} = g_{rr} + \theta'(r)^2$.

We consider the $U(1)$ world-volume gauge field A_μ , which is dual to the conserved current J^μ of the charge carriers. To have an electric field E_b only along the x^+ direction, we choose the gauge fields as

$$A_+ = \frac{E_b}{2\pi\ell_s^2}y + h_+(r), \quad A_- = \frac{b^2 E_b}{\pi\ell_s^2}y + h_-(r), \quad A_y = \frac{E_b b^2}{\pi\ell_s^2}x^- + h_y(r). \quad (5)$$

The light-cone electric field is a vector. We turn it on in one direction only (the y direction above). The system, however, is rotationally invariant despite appearances for reasons that are explained in appendix A.1, along with more detailed calculation of the transport. The resulting probe DBI action has the form

$$S_{D7} = -N_f T_{D7} \int d^8 \xi \sqrt{-\det(g_{D7} + 2\pi\ell_s^2 F)}, \quad (6)$$

where T_{D7} , ξ and F are the D-brane's tension, the world-volume coordinate and the $U(1)$ field strength, respectively.

There are three constants of motion, which we identify as three currents $\langle J^\mu \rangle = \frac{\delta \mathcal{L}}{\delta h'_\mu}$, where $\mu = +, -$ and y . We solve the equations of motion in terms of these currents, and obtain the on-shell action along the lines of [55]. Furthermore, we demand the square root in the action to be real all the way from the horizon, located at $r = r_H$, to the boundary at infinity. As shown in appendix A.1, it delivers two important relations:

$$\langle J^- \rangle = -\frac{g_{+-}(r_*)}{g_{--}(r_*)} \langle J^+ \rangle, \quad (7)$$

and Ohm's law, $\langle J^y \rangle = \sigma E_b$, with

$$\sigma = \sigma_0 \sqrt{\frac{J^2}{t^2 A(t)} + \frac{t^3}{\sqrt{A(t)}}}, \quad A(t) = t^2 + \sqrt{1 + t^4}. \quad (8)$$

where $\sigma_0 = \mathcal{N}b \cos^3 \theta \sqrt{2bE_b}$, and we use the dimensionless scaling variables

$$t = \frac{\pi \ell T b}{\sqrt{2bE_b}}, \quad J^2 = \frac{64\sqrt{2}\langle J^+ \rangle^2}{(\mathcal{N}b \cos^3 \theta)^2 (2bE_b)^3}. \quad (9)$$

Equation (8) is particularly interesting in the regime $t \ll 1$, $J \gg 1$;

$$\rho = \frac{1}{\sigma} \approx \frac{t}{J\sigma_0} = \frac{\pi \ell b \sqrt{E_b b}}{\langle J^+ \rangle} T. \quad (10)$$

Therefore, the Ohmic resistivity is linear in temperature in the low- T regime of the model.

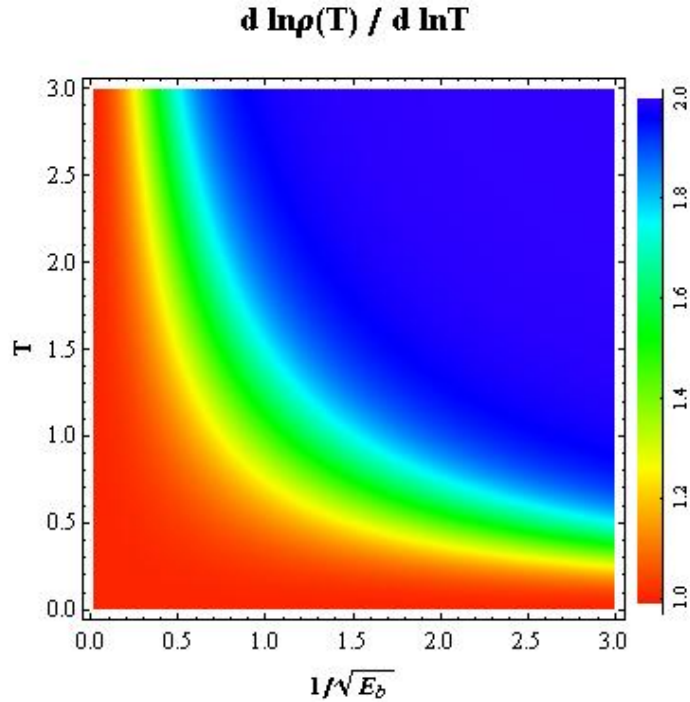


Figure 1: The exponent of $\frac{d \ln \rho(T)}{d \ln T}$ as a function of a tuning parameter $\frac{1}{\sqrt{E_b}}$ and temperature T at low temperatures. Note that the linear temperature dependence of the resistivity extends over the low temperature range, with $\rho \sim T + T^2$. Compare this plot to Fig. 3 of [18].

We now focus on the first term of eq. (8). At low temperatures, this term dominates over the second one, namely when $t \ll J^{\frac{1}{3}}$, $J \gg 1$. Notably, the first term is due to the drag

force exerted by the medium on heavier charge carriers (drag limit) [55]. In this limit, the resistivity reads

$$\rho \approx \frac{t}{J\sigma_0} \sqrt{t^2 + \sqrt{1+t^4}}. \quad (11)$$

The drag mechanism here is purely stringy and is explained below in subsection 4.1.

By increasing the scaling variable t , the temperature dependence of the resistivity crosses from linear $\rho \approx \frac{t}{J\sigma_0}$ to quadratic $\rho \approx \frac{\sqrt{2} t^2}{J\sigma_0}$. This crossover is governed by the bulk parameter b , setting the scale of the Lifshitz symmetry. E_b , on the other hand, is a more interesting parameter. Its direct physical interpretation is not straightforward as it is the light-cone component of an electric field in the boost direction x . In section 4.2, we also explain the interpretation of E_b and discuss why we expect $E_b \rightarrow 0$ to correspond to the heavily overdoped region whereas $E_b \rightarrow \infty$ to optimal doping. The crossover behavior observed is due to the fact that effectively the gravitational background (2), interpolates between $z=1$ (AdS) symmetry in the UV to $z=2$ Lifshitz symmetry in the IR.

4.1 Strong-coupling transport mechanisms

We will now comment on the resistivity results discussed in the previous section.

In strongly coupled systems described holographically, the conductivity of charge carriers has typically two contributions (that add quadratically), the “drag” term and the “pair-creation” term [55].

The physical picture corresponding to the drag contribution is that a charged “quark” moves through the strongly coupled (glue) plasma dragging behind its flux that is represented in the (fundamental) string. The “string” should be considered as the glue field attached to the “quark”. There is a world-volume horizon on that string, which has been interpreted to separate the part of the tail that has thermalized via interactions with the plasma and that is closer and follows the “quark”. It is losing energy because of the strong interactions with the plasma.

A Drude-like formula relates this energy loss and terminal velocity to the conductivity (drag conductivity). Although the Drude formula is classical and its physics are well understood, the result of the energy loss at strong coupling is poorly understood. The same mechanism for QCD is more or less experimentally tested in heavy-ion collisions. However, there is no alternative theoretical understanding of the dependence of the energy loss on terminal velocity, etc., apart from general symmetry considerations. The clear picture exists in the gravitational description: the resistance is due to the energy loss of a string moving in the appropriate gravitational background.

The other contribution is expected to be due to light charged pairs created from the vacuum contributing to the conductivity. This contribution is Boltzmann suppressed and controlled, in our model (and in [55]), by the coefficient \mathcal{N} given in equations (8) and (9) above. In full blown holographic models, this depends explicitly on the UV mass of charge carriers. Notably, this contribution comes from strong coupling and no alternative calculations of this exist in the same regime for comparison. This term picks up at higher temperatures and is not relevant to the regimes discussed below. Here, we are interested in the very low temperature regime to study the possible presence of quantum criticality and the associated superconducting mechanism.

Therefore, the model includes a bulk geometry representing critical “glue” that crosses over from $z=1$ to $z=2$ behavior in the IR and massive charge carriers (as probes) moving in this background, losing energy via the “drag” strong coupling mechanism.

4.2 The role and interpretation of the parameter E_b

The parameter E_b controls the physics of charge transport in analogy to experimental tuning parameters such as charge carrier doping, pressure, electric field or in-plane magnetic field.

A priori, E_b is a light-cone electric field component, $E_b = F_{+y}$. More precisely, as detailed in appendix A.1, it is a vector with two components, $E_b^y = F_{+y}$ and $E_b^z = F_{+z}$. However, as shown there, we may set $E_b = \sqrt{(E_b^y)^2 + (E_b^z)^2}$ and describe the transport properties in terms of E_b without loss of generality.

In the same appendix we also show that, despite the fact that the vector light-cone electric field is non-zero, transport is in fact rotationally invariant.

Since E_b is the only non-zero electric field component and, in particular, does not break rotational invariance in the transverse y, z directions, its presence demands an interpretation. Such an electric field can be obtained by an infinite boost along the x directions from a standard electric field E_y in the y direction. Under a boost $\lambda = \tanh \frac{v}{c}$ along the x direction,

$$F'_{+y} = \frac{\lambda}{2} E_y \quad , \quad F'_{-y} = \frac{1}{2\lambda} E_y \quad .$$

Therefore, to arrive at our set-up we need to send $\lambda \rightarrow \infty$ and $E_y \rightarrow 0$ so that the product is finite

$$E_b = \lim_{\substack{\lambda \rightarrow \infty \\ E_y \rightarrow 0}} \frac{\lambda}{2} E_y$$

Therefore, a non-zero E_b reflects an infinite boost of the system in the x direction and an infinitesimal electric field in the y direction. This limiting procedure explains why we should

not expect rotational invariance in the y - z plane to be broken as demonstrated explicitly in appendix A.1.

To interpret the effect of varying E_b , we will have to follow it through the passage to the infinite momentum frame. This translates into varying the "speed of light" c that enters in the boost. Therefore, fixing the same infinitesimal E_y in the rest frame and varying the "speed of light" is equivalent to varying E_b in the infinite momentum frame - in particular as $c \rightarrow 0$, $E_b \rightarrow \infty$. In our metric, this variation is implemented by varying the IR scale b that controls the passage between $z=1$ and $z=2$ scaling in the bulk geometry. This is also visible in all our expressions for the conductivity, in terms of the scaling variables where E_b appears always in the combination bE_b . Therefore, E_b should not be thought as an external field but as an internal variable parameter of the system.

By the relativity principle, we conclude that the infinite momentum frame captures the physics of charge carriers in two regimes:

- (a) The $z = 1$ CFT regime when $t = \frac{\pi \ell T b}{\sqrt{2bE_b}} \gg 1$.
- (b) The $z = 2$ Lifshitz-like regime when $t = \frac{\pi \ell T b}{\sqrt{2bE_b}} \ll 1$.

The transition temperature is controlled by E_b . $E_b \rightarrow 0$ maps to the large "doping" region where the resistivity is quadratic at all scales. This is the quadratic resistivity of CFT and is not necessarily associated, as is now well known, to fermions or bosons (in the $N = 4$ example, it is both.) $E_b \rightarrow \infty$ maps to optimal doping where the resistivity is linear at all scales.

There are several side arguments that support this map.

1. In parametrizing the resistivity as $\rho = a_1 T + a_2 T^2$ at low temperature, experiments indicate a_2 to be constant and a_1 to decrease rapidly with doping [18]. In our model, a_2 is indeed independent of E_b , while $a_1 \sim \sqrt{E_b}$ and vanishes across the "overdoped regime" ($E_b \rightarrow 0$).

2. The scaling variable for the magnetic field is $\mathcal{B} \sim \frac{B_b}{E_b}$ and the conductivities depend on \mathcal{B} alone. This is in accordance with experimental observations, where as one moves to the overdoped region the effects of the magnetic field are stronger [28]. This is discussed in more detail below. Notably, in the families of strange metals one may vary the chemical potential also using an external magnetic and electric field and not necessarily chemical doping.

It is not entirely clear at the moment how parameters such as the "internal light velocity" (as defined by the holographic metric) is related to standard physical properties of the material - charge density, velocity of quasiparticles, etc. To assert this, a more detailed analysis is necessary where several new constituents should be considered - for instance, the calculation of correlation functions of currents, couplings to fermions, and potentially others.

This analysis maybe necessary to provide further features for this class of ideas. However, it is beyond the focus of the present effort.

5 Holographic Hall transport

In this section, we analyze the charge transport in the presence of a magnetic field following [56]. The detailed calculation is carried out in appendix A.2. The analysis of the behavior of the conductivity in different regimes can be found in appendix B.

The gauge fields now are

$$A_+ = \frac{E_b}{2\pi\ell_s^2}y + h_+(r), \quad A_- = \frac{b^2 E_b}{\pi\ell_s^2}y + h_-(r), \quad A_y = \frac{E_b b^2}{\pi\ell_s^2}x^- + h_y(r), \quad A_z = \frac{B_b y}{2\pi\ell_s^2} + h_z(r). \quad (12)$$

This configuration includes a light-cone electric field, E_b , along the y direction and a magnetic field, B_b , perpendicular to the y, z directions. The DBI probe action eq. (6) has four conserved currents, $\langle J^\mu \rangle$, related to the variation of $h'_\mu(r)$ with $\mu = +, -, y$ and z . The exact Ohmic conductivity in the presence of a magnetic field is

$$\sigma^{yy} = \sigma_0 \frac{\sqrt{\mathcal{F}_+ J^2 + t^4 \sqrt{\mathcal{F}_+ \mathcal{F}_-}}}{\mathcal{F}_-}, \quad \sigma^{yz} = \bar{\sigma}_0 \frac{\mathcal{B}}{\mathcal{F}_-}, \quad (13)$$

where $\bar{\sigma}_0 = \frac{\langle J^+ \rangle}{bE_b}$, σ_0 was defined earlier (eq. (8)), and t, J in eq. (9). Here

$$\mathcal{F}_\pm = \sqrt{(\mathcal{B}^2 + t^4)^2 + t^4} \mp \mathcal{B}^2 + t^4, \quad \mathcal{B} = \frac{B_b}{2bE_b}. \quad (14)$$

Note that eqs. (13) and (14) reduce to eq. (8) for $\mathcal{B} = 0$.

For a rotationally symmetric system with a plane of y, z coordinates, the resistivity matrix is defined as the inverse of the conductivity matrix. The inverse Hall angle is defined as the ratio between Ohmic conductivity and the Hall conductivity as $\cot \Theta_H = \frac{\sigma^{yy}}{\sigma^{yz}}$. We also define the Hall coefficient R_H and the magnetoresistance $\frac{\Delta\rho}{\rho}$ as

$$R_H = \frac{\rho_{yz}}{B}, \quad \frac{\Delta\rho}{\rho} = \frac{\rho_{yy}(B) - \rho_{yy}(0)}{\rho_{yy}(0)}. \quad (15)$$

For J sufficiently large, the resistivities are given by drag contributions. There are three relevant regimes:

(a) $\mathcal{B} \ll t \ll 1$ with

$$R_H \simeq \frac{\bar{\sigma}_0}{\sigma_0^2 J^2}, \quad \cot \Theta_H \simeq \frac{\sigma_0 J}{\bar{\sigma}_0 \mathcal{B} t}, \quad \frac{\Delta\rho}{\rho} \simeq \frac{3}{2} \frac{\mathcal{B}^2}{t^2}, \quad (16)$$

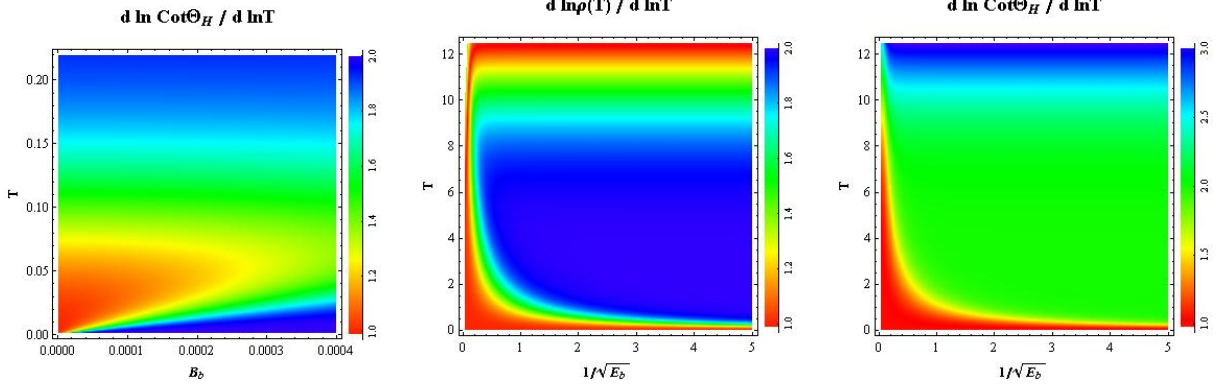


Figure 2: Left: Temperature (T) and magnetic field (B) dependence of the exponent of $\cot \Theta_H$ in the low T , low B regions. Middle: The effective power n of the resistivity $\rho \sim T^n$ at zero magnetic field as a function of temperature (T) and the effective doping parameter $1/\sqrt{E_b}$. For $T \lesssim 8$, the resistivity is dominated by the drag mechanism, while at $T \gtrsim 8$ it is dominated by the pair-creation term. Right: the effective power dependence of $\cot \Theta_H$ at small magnetic field, as a function of temperature and $1/\sqrt{E_b}$. For $T \lesssim 8$, the resistivity is dominated by the drag mechanism, while at $T \gtrsim 8$ it is dominated by the pair-creation term. Note that here the range of the power varies from 1 to 3.

(b) $\mathcal{B} \ll t^2$ and $t \gg 1$ with

$$R_H \simeq \frac{\bar{\sigma}_0}{\sigma_0^2 J^2}, \quad \cot \Theta_H \simeq \frac{\sqrt{2}\sigma_0 J}{\bar{\sigma}_0 \mathcal{B}} t^2, \quad \frac{\Delta \rho}{\rho} \simeq \frac{\mathcal{B}^2}{t^4}, \quad (17)$$

(c) $\mathcal{B} \gg t$ and $\mathcal{B} \gg t^2$ with

$$R_H \simeq \frac{2}{\bar{\sigma}_0}, \quad \cot \Theta_H \simeq \frac{\sigma_0 J \sqrt{1 + 4\mathcal{B}^2}}{\bar{\sigma}_0 \sqrt{2}\mathcal{B}} t^2, \quad \frac{\Delta \rho}{\rho} \simeq \frac{2\sqrt{2}\sigma_0^2 J^2 t^2}{\bar{\sigma}_0^2 t \mathcal{A}}. \quad (18)$$

For a summary of these properties we refer the reader to Fig. 2.

The above-mentioned transport properties can be compared successfully to those of strange metals as described in the section below.

6 Comparison to experiment

Since the discovery of the high T_c cuprate superconductors 25 years ago, there have been significant experimental efforts to identify the physical mechanism governing their unconventional superconducting and normal state properties. Magnetotransport has been at the heart of studying the emerging properties of superconductors. Here, we focus our discussion

on characteristic quantities which have puzzled the condensed matter community and remain largely unexplained. We discuss especially the region where the concentration of charge carrier doping is sufficiently high to span the phase diagram from optimal superconductivity (optimal doping) towards its suppression due to excessive carrier concentration (overdoping). For this we chose to address two prototypical copper oxide superconductors, namely $La_{2-x}Sr_xCuO_4$ (LSCO) and $Tl_2Ba_2CuO_{6+\delta}$ (TBCO), for which it is possible to span the abovementioned doping range. The normal state of these superconductors may be accessed by suppressing superconductivity, for example, through the substitution of Zn for Cu (see *e.g.*, [22, 23, 29]) or by a sufficiently high applied magnetic field [34, 18]. For a nice review concerning anomalous transport properties of cuprates, see *e.g.*, [17].

It has been generally accepted that at optimal doping i.e., where the absolute value of the superfluid density is highest, the resistivity in the normal state of cuprate superconductors varies linearly with T . This unconventional behavior has often been discussed in terms of quantum criticality. As charge carrier doping increases, the linearity gives way to higher power laws and eventually a more or less Fermi liquid regime emerges. However, recent low temperature transport data [18] on LSCO have challenged earlier works [57]. In [18], the authors reported that the suppressed superconducting region is replaced by a "2D strange metal", with the Ohmic resistivity at low temperature behaving as $\rho \sim T + T^2$. Especially the doping region where the resistivity varies linearly with T is broader than expected and continues to survive in the heavily overdoped side of the phase diagram. This result suggests a line of critical points and therefore a significant departure from our earlier understanding on the possible role of the above mentioned linearity and a well defined, singular quantum critical point coinciding with optimal superconductivity. This result is in fact consistent with an earlier observation on TBCO at very low temperatures $T < 30K$ - see Figs 5 and 6 in [19]. Notably, a line of critical points has recently been argued for another group of unconventional superconductors on the border of magnetism, namely the f -electron systems [39].

The inverse Hall angle has been shown to vary as $\cot \Theta_H \sim T + T^2$ at very low temperatures in TBCO [19], which is surprising on the basis of the conventional wisdom considering two scattering rates in the cuprate superconductors. In particular, the inverse Hall angle and the resistivity behave in a similar manner, namely as $\cot \Theta_H \sim \rho \sim T + T^2$ at very low temperature, $T < 30$. This is clearly depicted in Fig. 9 of [19]. It has been argued that two scattering rates observed in the overdoped region of TBCO collapse on to a single scattering rate as $T \rightarrow 0$, in the temperature range $T < 30K$ [19]. The similar behavior between resistivity and inverse Hall angle might be considered to be the realm of a Fermi liquid, yet their strong linear temperature dependence over a broad range of doping is a challenge [19][18][57]. For LSCO, similar behaviors were observed for the inverse Hall angle

[25].

Here, we compare the results of our model with the experimental results. We focus our attention on several key and outstanding features of the normal state of cuprate superconductors. Namely, the analysis of the in-plane resistivity, in-plane Hall coefficient, inverse Hall angle, in-plane magnetoresistance and the modified Köhler rule. We start by summarizing the main features of the transport properties described by our model.

1. In the absence of an applied magnetic field, there is a linear resistivity near $T = 0$, which changes to quadratic at higher temperatures. The coefficient of the quadratic term is independent of E_b , whereas that of the linear term is proportional to $\sqrt{E_b}$, which is directly related to the inverse of the doping.
2. In the presence of a magnetic field, $\cot \Theta_H$ is linear when the resistivity is linear, and quadratic when the resistivity is quadratic. This is the behavior seen in strange metals at very low temperatures (for example below 25 K in overdoped $Tl_2Ba_2CuO_{6+\delta}$). At higher temperatures however, the quadratic behavior in real materials dominates the overdoped side.
3. The magnetoresistance calculated is in agreement with experimental data at low temperatures. The model predicts that near $T = 0$ the magnetoresistance dives sharply towards zero.
4. The universal scaling behavior of Hall coefficient, available in the experimental literature, is qualitatively very similar to the scaling function $\frac{1}{t\sqrt{A}}$ of our model.
5. The “modified Köhler” rule is known to be valid for cuprates and other related materials. Köhler’s rule has been shown experimentally to fail at relatively high temperatures in the overdoped region. It has been argued that this is due to a superconducting instability [58]. We show that it is also compatible with the correlation between $\cot \Theta_H$ and resistivity as observed experimentally at low temperatures. The model therefore predicts that at sufficiently low temperatures both the Köhler and modified Köhler rules are valid in the overdoped region.

6.1 Resistivity

Let us concentrate on the recent experimental observations on LSCO and TBCO at very low temperature. In overdoped TBCO the resistivity in the millikelvin regime follows $\rho \sim T + T^2$ [19]. Recently, very low temperature resistivity data on LSCO over a wide range of

doping, namely from slight underdoped $p = 0.15$ to heavily overdoped $p = 0.33$, indicate that the suppressed superconducting region in the overdoped regime has an unexpected $\rho = a_0 + a_1T + a_2T^2$ behavior, with a particularly interesting linear temperature dependence of the resistivity at very low temperatures [18]. Furthermore, a_2 was found to be doping independent, while a_1 decreased rapidly with overdoping. Earlier works in the overdoped region (above $p \sim 0.2$) for LSCO reported a novel power-law $\rho = \rho_0 + AT^n$ with $n \sim 1.5$ dominating the resistivity over a wide temperature range (see for example, Fig. 1 in [23]). Here we make a comparison of our results to the abovementioned reports.

We focus on the drag limit mentioned above. The drag term, proportional to J^2 in eq. (6), dominates in the low temperature limit. Here, the resistivity has two different contributions, one linear in T and another T^2 ,

$$\rho \approx a_1T = \left(\frac{\sqrt{E_b/b}}{\ell\pi} \right) \frac{\ell^2\pi^2b^2}{\langle J^+ \rangle} T, \quad \rho \approx a_2T^2 = \frac{\ell^2\pi^2b^2}{\langle J^+ \rangle} T^2. \quad (19)$$

a_2 is doping independent whereas a_1 decreases rapidly with doping, in agreement with our model. We may therefore, map $\frac{1}{\sqrt{E_b}}$ to the doping parameter as depicted above in Fig. 1.

6.2 Inverse Hall angle

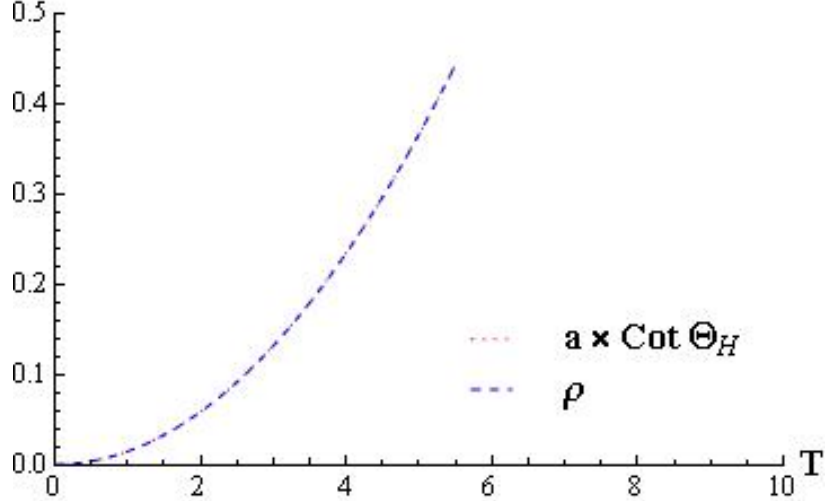


Figure 3: Plot of the resistivity and inverse Hall angle, in our model, for the low-temperature regime with small magnetic field. Note that the inverse Hall angle has been scaled by a constant factor $a = B_b/(32\sqrt{2}\langle J^+ \rangle)$. This plot is to be compared with Fig. 9 of [19].

The inverse Hall angle is defined as $\cot \Theta_H = \sigma_{yy}/\sigma_{yz}$. At optimal doping and relatively high temperature ($T \geq 100K$ for YBCO [22], LSCO [25] and TBCO [21]), $\cot \Theta_H$ varies universally as T^2 , while the corresponding Hall coefficient is highly irregular. To the best of our knowledge there is no corresponding systematic data available for optimal doping at very low temperatures.

The first observation of $\cot \Theta_H = T + T^2$ in overdoped samples at low temperatures is depicted in Fig. 8 of [19]. Notably, the resistivity and the inverse Hall angle for TBCO behave in a similar manner at low temperature (Fig. 9 of [19]). There is also indirect evidence for universality from works on LSCO see *e.g.*, Fig. 3 of [59] and Fig. 3 (c) of [60]. Further support may be obtained from earlier studies on overdoped LSCO. For instance, in [25] the authors suggest $\cot \Theta_H$ cannot be fitted by $A + BT^2$ in the range $T = 4K$ to $T = 500K$ (Fig. 4 in [25]). A thorough investigation at very low temperature however, has yet to be performed.

Our results demonstrate that the resistivity and the inverse Hall angle behave in a similar manner when the system is at low temperature and small magnetic fields, indicating that we are working in a linear regime or a weak field regime as defined by the experimental results for the magnetoresistance $\frac{\Delta\rho}{\rho} \sim B_b^2$ and Hall coefficient $R_H \sim B_b^0 \sim \text{const.}$ [28]. This is depicted in Fig. 3.

6.3 Magnetoresistance

The magnetoresistance is defined as follows:

$$\frac{\Delta\rho}{\rho} \equiv \frac{\rho_{yy}(B) - \rho_{yy}(0)}{\rho_{yy}(0)}. \quad (20)$$

Unlike overdoped TBCO ($T_c \sim 30$ K), in optimally doped TBCO ($T_c \sim 80$ K) the weak magnetic field regime extends up to 60 T. This has implications on the doping dependence of \mathcal{B} . The scaling dependence of the resistivity on magnetic field, via the scaling in equation (14) is in qualitative agreement with experimental results [28]. Hence, magnetic fields, which are in the linear regime at optimal doping are in fact in the non-linear regime in the overdoped region (optimal doping here is $E_b \rightarrow \infty$).

The magnetoresistance in heavily overdoped TBCO increases gradually with decreasing T , approaching a finite value at the lowest temperatures measured, around 30K, in the low temperature and weak field regime (being proportional to square of magnetic field); see Fig. 1 of [27]. This behavior is captured by our results, as depicted in Fig. 4. We expect the strong dip as $T \rightarrow 0$ may be also visible if experiments at lower temperatures are performed.

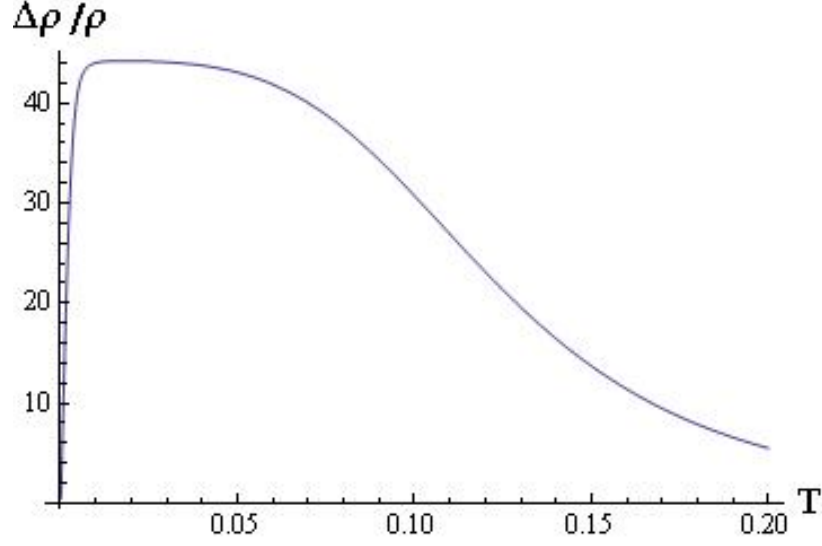


Figure 4: The plot depicts the magnetoresistance for a heavily overdoped sample at lower temperature, which is to be contrasted to Fig. 1 of [27].

6.4 Hall coefficient

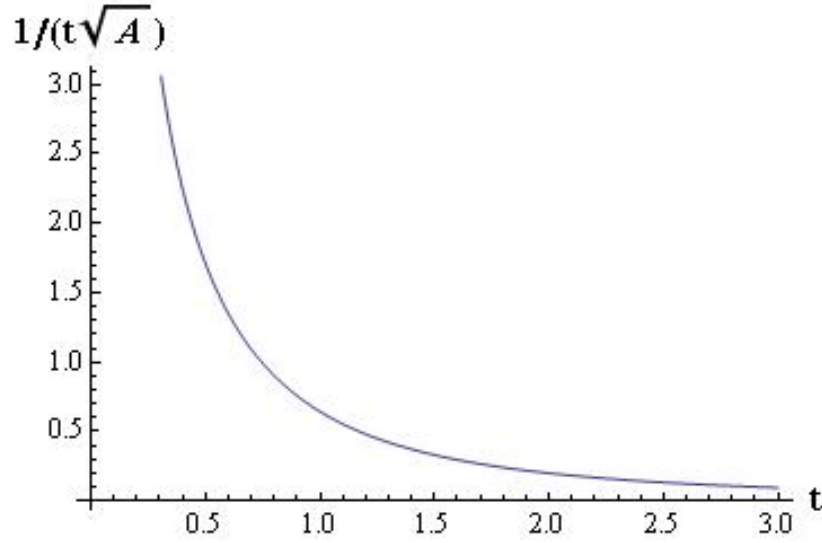


Figure 5: Temperature dependence of the normalized Hall coefficient. This corresponds to the function $\frac{1}{t\sqrt{A}}$ of our model. Compare this to the plot of the quantity, $\frac{R_H(T/T_*) - R_H(\infty)}{R_H^*}$, Fig. 2 of [25].

Attempts to identify a universal scaling behavior for the Hall coefficient in cuprate superconductors have not been very successful [22]. On the other hand, the inverse Hall angle

depicts a universal behavior [22]. It has been argued however, that the central anomaly of the Hall effect resides in direct measurements of the Hall coefficient [61].

To the best of our knowledge, there is only one report where a scaling behavior of the Hall coefficient $\frac{R_H(T/T^*) - R_H(\infty)}{R_H^*}$, was argued to show a universal scaling behavior [25]. Here, $R_H(\infty)$ is the high temperature limit of R_H , R_H^* rescales the magnitude, and T^* is a temperature scale. The scaling behavior is shown in Fig. 2 of [25]. We compare this result to $\frac{1}{t\sqrt{A}}$ of our model, which can be shown to be the Hall coefficient at a vanishingly small B with only temperature scaling. This is presented on Fig. 5.

6.5 Köhler rule

Köhler's rule for metals states that $K = \rho^2 \frac{\Delta\rho}{\rho}$ should be independent of temperature. This was claimed to fail for YBCO and LSCO [26]. The authors of [26] suggested, however, that a modified Köhler rule is valid and $(\cot \Theta_H)^2 \frac{\Delta\rho}{\rho}$ is approximately constant with temperature.

It has been argued that for LSCO superconducting fluctuations play an important role in accounting for the difference between Köhler's rule and the modified Köhler rule [58]. While in principle our model can be shown to exhibit a superconducting transition by coupling to gauge and scalar fields, in the current setup our system does not include superconducting fluctuations. Furthermore, at very low temperatures in the overdoped regime we do not expect that two such scales exist, as suggested by the very low temperature measurements of magnetoresistance.

Our data for the Köhler ratio and the modified Köhler ratio are in general temperature dependent, but not in the small temperature and large temperature limits. Indeed, the facts that the resistivity and the inverse Hall angle are proportional at low temperatures and the modified Köhler ratio is constant implies that the Köhler ratio is also constant at very low temperatures. Although this seems to be in contradiction with claims in the literature, we believe it should be valid at very low temperatures, in view of the proportionality of $\cot \Theta_H$ to ρ [19].

7 Outlook

A simple holographic system, namely the AdS-Schwarzschild black hole in light-cone coordinates, provides a solvable quantum critical model of magnetotransport with a wide range of properties. The results obtained are in good agreement with those of strange metals, in particular the high- T_c cuprates at very low temperatures with charge carrier concentration

ranging from the optimal to the overdoped regime. An intriguing novel property emerging from our work is the scaling of the carrier doping dependence, hence, the model at $T = 0$ should be considered as a quantum critical line albeit with a Lifshitz scaling of $z=2$, which presents a radical departure from the paradigm of the isolated critical point. This controls the linear resistivity in this regime as suggested in [42]. Recent experimental results also point in this direction. This regime crosses over to a quadratic one, controlled by a standard CFT liquid. The crossover temperature diverges at optimal doping $E_b \rightarrow \infty$ explaining the high temperature reach of the linear resistivity regime.

Moreover, our findings provide several novel experimental and testable signatures for the low-temperature behavior of strange metals.

- The magneto-resistance vanishes abruptly near $T = 0$.
- At sufficiently low temperatures, the transport data scale with a function B/B_* , where B_* is doping dependent.
- The Köhler rule and modified Köhler rule are both valid at low temperatures.

An extension to this work would be to clarify the underlying dynamics and how it matches the expected interactions of electrons in real materials.

The precise relation of the holographic model presented here with microscopic dynamics has yet to be clarified. Ideas in this direction have already been discussed [62] and connected to critical points and phases of the Hubbard model in [63]. They are based on expectations of emergent strong non-abelian interactions at low energies and the ensuing holographic description. However, the non-standard holographic realization of the non-relativistic scaling symmetries remains a generic puzzle. The emergence of superconductivity in this context is another important direction to be explored. For instance, using a probe scalar and gauge fields one would be able to study the onset of superconductivity and its dependence on quantum tuning parameters including charge carrier doping and magnetic field.

Acknowledgments

We would like to thank T. Hu, M. Lippert, A. O'Bannon and D. Yamada for discussions. This work has been partially supported by grants MEXT-CT-2006-039047, EURYI, FP7-REGPOT-2008-1-CreteHEPCosmo-228644, PERG07-GA-2010-268246 and the National Research Foundation, Singapore.

Appendix

A Detailed calculation of the conductivity

A.1 Conductivity calculation with E_b^y and E_b^z

In this section, we calculate the conductivity tensor in the absence of a magnetic field, and in the presence of arbitrary E_b^y and E_b^z . In this way we will also check that the system remains rotationally symmetric. The calculation is done in the probe approximation⁴ following [55]. We confirm that the light-cone electric field we turn on does not break rotational invariance. Therefore, in the main part of the paper E_b should be taken as $\sqrt{(E_b^y)^2 + (E_b^z)^2}$.

For our purposes, we consider the ansatz

$$\begin{aligned} A_+ &= E_b^y y + E_b^z z + h_+(r), & A_- &= b^2 E_b^y y + b^2 E_b^z z + h_-(r), \\ A_y &= b^2 E_b^y x^- + h_y(r), & A_z &= b^2 E_b^z x^- + h_z(r), \end{aligned} \quad (21)$$

With these gauge fields, we have light-cone electric fields along y, z directions. For simplicity we set $2\pi\ell_s^2 = 1$ and ignore the contribution from the extra dimensions of S^5 as they are not relevant.

The DBI action is

$$S_{D7} = -\mathcal{N} \int dr \sqrt{-\det(g_{\mu\nu} + F_{\mu\nu})} = -\mathcal{N} \int dr \sqrt{-\det M}, \quad (22)$$

where $F_{\mu\nu} = \partial_\mu A_\nu - \partial_\nu A_\mu$ and

$$\begin{aligned} \det M &= g_{--} (E_b^z h'_y - E_b^y h'_z)^2 + G_{+-} g_{yy} (h_y'^2 + h_z'^2) + ((E_b^y)^2 + (E_b^z)^2) g_{xx} (g_{rr} g_{--} + h_-'^2) \\ &\quad + g_{xx}^2 (G_{+-} g_{rr} + g_{--} h_+'^2 + h_-' (-2g_{+-} h_+' + g_{++} h_-')) , \end{aligned} \quad (23)$$

with

$$G_{+-} = -g_{+-}^2 + g_{++} g_{--}, \quad G_{+-y} = ((E_b^y)^2 + (E_b^z)^2) g_{--} + G_{+-} g_{xx}. \quad (24)$$

and the metric coefficients are defined in (2).

⁴This is a good approximation strictly speaking when the number of flavors remains fixed as the number of colors is large.

Varying the gauge fields, we obtain the constants of motion, (that are the currents)

$$\begin{aligned}
\langle J^+ \rangle &= \bar{H} \ , \quad \bar{H} = -\mathcal{N}/\sqrt{-\det M} g_{yy}^2 (g_{--} h'_+ - g_{+-} h'_-) \ , \\
\langle J^- \rangle &= -\bar{H} g_{yy} (-g_{+-} g_{yy} h'_+ + ((E_b^y)^2 + (E_b^z)^2 + g_{++} g_{yy}) h'_-) \ , \\
\langle J^y \rangle &= \bar{H} (G_{+-} g_{yy} A'_y + (E_b^z) g_{--} ((E_b^z) A'_y - (E_b^y) A'_z)) \ , \\
\langle J^z \rangle &= \bar{H} (G_{+-} g_{yy} A'_z + (E_b^y) g_{--} (-(E_b^z) A'_y + (E_b^y) A'_z)) \ ,
\end{aligned} \tag{25}$$

One solves the equations (25) and substitute the solution back into the action to obtain the on-shell action

$$S_{D\tau} = -\mathcal{N}^2 \int dr g_{yy} \sqrt{g_{rr}} \sqrt{\frac{G_{+-y}}{-g_{yy} \mathcal{N}^2 - \bar{U} - \bar{V}}} \ , \tag{26}$$

where

$$\bar{U} = \frac{(\langle J^y \rangle E_b^y + \langle J^z \rangle E_b^z)^2 g_{--} + (\langle J^z \rangle^2 + \langle J^y \rangle^2) G_{+-} g_{yy}}{G_{+-} G_{+-y}} \ , \tag{27}$$

$$\bar{V} = \frac{\langle J^+ \rangle^2 ((E_b^y)^2 + (E_b^z)^2) + \langle J^+ \rangle^2 g_{++} g_{yy} \langle J^- \rangle \{2\langle J^+ \rangle g_{+-} + \langle J^- \rangle g_{--}\} g_{yy}}{G_{+-y} g_{yy}} \ . \tag{28}$$

and where $\langle J^\pm \rangle, \langle J^{y,z} \rangle$ are constants and

$$G_{+-y}(r) = ((E_b^y)^2 + (E_b^z)^2) g_{--}(r) + G_{+-} g_{xx}(r) \ . \tag{29}$$

As r varies from the boundary of the geometry to the horizon, both the numerator and denominator in the square root in (26) decrease and at some point change sign from positive to negative. Consistency for the solution implies that they should change sign at the same radial distance [55]. We call r_* the value of r where this numerator changes the sign $G_{+-y}(r_*) = 0$. The functions \bar{U}, \bar{V} have vanishing denominators, and therefore we demand $\bar{U}(r_*) = \bar{V}(r_*) = 0$ at least as fast as G_{+-y} . These conditions imply

$$\langle J^- \rangle = -\frac{g_{+-}}{g_{--}} \Big|_{r=r_*} \langle J^+ \rangle \ , \quad \langle J^z \rangle = \frac{-E_b^y E_b^z g_{--}}{(E_b^z)^2 g_{--} + G_{+-} g_{yy}} \Big|_{r=r_*} \langle J^y \rangle \ . \tag{30}$$

Substituting this condition in the action and demanding that the denominator is zero at $r = r_*$, we obtain the current along the y direction. This equation gives

$$\langle J^y \rangle^2 = (E_b^y)^2 \frac{(\langle J^+ \rangle^2 + \mathcal{N}^2 g_{--} g_{yy}^2)}{g_{yy}^2} \Big|_{r=r_*} \ , \tag{31}$$

where we used $G_{+-y} = 0$ at $r = r_*$. From equation (30), we obtain

$$\langle J^z \rangle^2 = (E_b^z)^2 \frac{(\langle J^+ \rangle^2 + \mathcal{N}^2 g_{--} g_{yy}^2)}{g_{yy}^2} \Big|_{r=r_*} \ . \tag{32}$$

From the definition of the conductivity

$$\langle J^i \rangle = \sigma_{ij} E_b^j, \quad (33)$$

and (31) and (32) we obtain

$$\sigma^{yy} = \sigma^{zz} = \sqrt{\left. \frac{(\langle J^+ \rangle^2 + \mathcal{N}^2 g_{--} g_{yy}^2)}{g_{yy}^2} \right|_{r=r_*}}, \quad \sigma^{yz} = \sigma^{zy} = 0. \quad (34)$$

Equation (34) is the same as equation (8) in the main text after redefinitions. It is clearly rotationally invariant with $(E_b^y)^2 + (E_b^z)^2 \longrightarrow E_b^2$.

A.2 Hall conductivity calculation

In the presence of a magnetic field, we will use the DBI probe technique developed in [56]. The calculations are similar to the previous section, yet more involved. Here we will present only the important steps in the calculation. We also take $2\pi\ell_s^2 = 1$ and ignore the contribution from the extra dimensions of S^5 because it is not relevant.

To calculate the Hall conductivity, we choose the following gauge fields

$$A_+ = E_b y + h_+(r), \quad A_- = 2b^2 E_b y + h_-(r), \quad A_y = 2b^2 E_b x^+ + h_y(r), \quad A_z = B_b y + h_z(r), \quad (35)$$

which are the same as equation (12). These gauge fields describe a light-cone electric field along the y direction and a magnetic field perpendicular to the $y - z$ plane.

The action is $S_{D7} = -\mathcal{N} \int dr \sqrt{-\det M}$, where

$$\begin{aligned} \det M = & G_{+-y} g_{rr}(r) + g_{yy}(r)^2 h'_+(r) (g_{--}(r) h'_+(r) - 2g_{+-}(r) h'_-(r)) \\ & + g_{--}(r) (B_b h'_+(r) - E_b h'_z(r))^2 + G_{+-} g_{yy}(r) (h'_y(r)^2 + h'_z(r)^2) \\ & + h'_-(r) (G_{+y} h'_-(r) + 2B_b g_{+-}(r) (-B_b h'_+(r) + E_b h'_z(r))) . \end{aligned} \quad (36)$$

and

$$\begin{aligned} G_{+-y} = & [B_b^2 + g_{yy}(r)^2] G_{+-} + E_b^2 g_{--}(r) g_{yy}(r), \quad G_{+-} = -g_{+-}(r)^2 + g_{++}(r) g_{--}(r), \\ G_{+y} = & B_b^2 g_{++}(r) + E_b^2 g_{yy}(r) + g_{++}(r) g_{yy}(r)^2. \end{aligned} \quad (37)$$

The constants of motion are (with simplified notation $h_+ = h_+(r)$)

$$\begin{aligned} \langle J^+ \rangle = & \bar{H} (-g_{+-} (B_b^2 + g_{yy}^2) h'_- + g_{--} ((B_b^2 + g_{yy}^2) h'_+ - B_b E_b h'_z)) , \\ \langle J^- \rangle = & -\bar{H} (G_{+y} h'_- - g_{+-} ((B_b^2 + g_{yy}^2) h'_+ - B_b E_b h'_z)) , \\ \langle J^y \rangle = & \bar{H} G_{+-} g_{yy} h'_y , \\ \langle J^z \rangle = & \bar{H} (B_b E_b g_{+-} h'_- + G_{+-} g_{yy} h'_z + E_b g_{--} (-B_b h'_+ + E_b h'_z)) , \end{aligned} \quad (38)$$

$$\text{where } \bar{H} = -\frac{\mathcal{N}}{\sqrt{-\det M}} .$$

We solve the equations (39) and substitute the solutions into the action, to obtain

$$S_{D_7} = -\mathcal{N}^2 \int dr \sqrt{\frac{g_{rr} G_{+-y}}{-\mathcal{N}^2 - \bar{W}(r) + \bar{U}(r) - \bar{V}(r)}}, \quad (39)$$

where

$$\begin{aligned} \bar{U}(r) &= \frac{-B_b^2 \langle J^+ \rangle^2 G_{+-}^2 + E_b g_{--} (E_b (\langle J^z \rangle B_b + \langle J^+ \rangle E_b)^2 g_{--} + \langle J^+ \rangle (2 \langle J^z \rangle B_b + \langle J^+ \rangle E_b) G_{+-} g_{yy})}{B_b^2 G_{+-} g_{--} (E_b^2 g_{--} g_{yy} + G_{+-} (B_b^2 + g_{yy}^2))}, \\ \bar{V}(r) &= \frac{-(\langle J^+ \rangle g_{+-} + \langle J^- \rangle g_{--})^2}{g_{--} (-G_{+-} g_{--} + g_{+-}^2 (B_b^2 + g_{yy}^2))}, \\ \bar{W}(r) &= \frac{(\langle J^z \rangle^2 + \langle J^y \rangle^2) B_b^2 + 2 \langle J^z \rangle \langle J^+ \rangle B_b E_b + \langle J^+ \rangle^2 E_b^2}{B_b^2 G_{+-} g_{yy}}. \end{aligned} \quad (40)$$

As before, we demand the square root factor to be real all the way from the horizon to the boundary. The numerator of the action changes sign at $r_H < r = r_* < \infty$ and we solve it explicitly as

$$\left[(g_{yy}(r)^2 + B_b^2) G_{+-} + E_b^2 g_{--}(r) g_{yy}(r) \right]_{r=r_*} = 0, \quad (41)$$

which implies

$$r_*^4 = \frac{1}{2} \left(r_H^4 - B_b^2 \ell^4 + \sqrt{(r_H^2 + \ell^4 B_b^2)^2 + 4 E_b^2 b^2 r_H^4 \ell^4} \right). \quad (42)$$

For the on-shell action to be real, the denominator should also vanish at $r = r_*$. It turns out that the functions $\bar{U}(r), \bar{V}(r)$ have also vanishing denominator. Thus we demand $\bar{U}(r_*) = \bar{V}(r_*) = 0$ at least as fast as G_{+-y} . Setting the numerators of \bar{V}, \bar{U} to be zero at $r = r_*$, we obtain

$$\langle J^- \rangle = - \frac{g_{+-}(r)}{g_{--}(r)} \Big|_{r=r_*} \langle J^+ \rangle, \quad (43)$$

$$\langle J^z \rangle = - \frac{E_b^2 g_{--}(r)^2 + G_{+-} g_{--}(r) g_{yy}(r)}{B_b E_b g_{--}(r)^2} \Big|_{r=r_*} \langle J^+ \rangle. \quad (44)$$

By plugging this condition to the denominator of the action, we obtain the expression of the current along y direction. In turn we use the Ohm's law to obtain

$$\sigma^{yy} = \frac{g_{yy}(r)}{B_b^2 + g_{yy}(r)^2} \sqrt{\langle J^+ \rangle^2 + \mathcal{N}^2 g_{--}(r) (B_b^2 + g_{yy}(r)^2)} \Big|_{r=r_*}. \quad (45)$$

This expression can be evaluated with explicit temperature dependence as

$$\begin{aligned} \sigma^{yy} &= \frac{\ell}{\mathcal{G}_-} \left(64 \sqrt{2} \langle J^+ \rangle^2 \mathcal{G}_+ + \ell^2 \mathcal{N}^2 \pi^4 T^4 b^6 \sqrt{\mathcal{G}_+ \mathcal{G}_-} \cos^6 \theta \right)^{1/2}, \\ \mathcal{G}_+ &= \ell^2 \sqrt{(B_b^2 + \pi^4 b^4 \ell^4 T^4)^2 + 4 \pi^4 E_b^2 b^6 \ell^4 T^4} - B_b^2 \ell^2 + \pi^4 b^4 \ell^6 T^4, \\ \mathcal{G}_- &= \ell^2 \sqrt{(B_b^2 + \pi^4 b^4 \ell^4 T^4)^2 + 4 \pi^4 E_b^2 b^6 \ell^4 T^4} + B_b^2 \ell^2 + \pi^4 b^4 \ell^6 T^4, \end{aligned} \quad (46)$$

where we used the identification $r_H = \ell^2 \pi T b$ and these expressions are the same as the equations (13) and (14) with appropriate identifications. When the magnetic field vanishes, this expression reduces to the conductivity formula given in equation (8), which provide a consistency check. The Hall conductivity can be calculated from (44) and (46) as

$$\sigma^{yz} = \frac{B_b \langle J^+ \rangle}{B_b^2 + g_{yy}(r)^2} = \frac{2\ell^2 B_b \langle J^+ \rangle}{\mathcal{G}_-}, \quad (47)$$

which is identical to the equation (13). This Hall conductivity vanishes when the magnetic field vanishes.

B Study of the temperature dependence of the conductivity.

In this appendix we would investigate the temperature dependence of the conductivity in various regimes in the presence of a magnetic field. The two main regimes are the drag dominant regime (at lower temperatures) and also the “pair creation” regime at higher temperatures.

The basic starting formulae are

$$\sigma_{yy} = \frac{\sigma_0}{\mathcal{F}_-} \sqrt{\mathcal{F}_+ J^2 + t^4 \sqrt{\mathcal{F}_+ \mathcal{F}_-}}, \quad \sigma_{yz} = \bar{\sigma}_0 \frac{\mathcal{B}}{\mathcal{F}_-}, \quad \cot \Theta_H = \frac{\sigma_{yy}}{\sigma_{yz}}, \quad (48)$$

$$\mathcal{F}_\pm = t^4 \left[1 \mp \frac{\mathcal{B}^2}{t^4} + \sqrt{\left(1 + \frac{\mathcal{B}^2}{t^4}\right)^2 + \frac{1}{t^4}} \right], \quad J^2 = \frac{64\sqrt{2}\langle J^+ \rangle^2}{(\mathcal{N}b \cos^2 \theta)^2 (2bE_b)^3}, \quad (49)$$

$$t = \frac{\pi \ell b T}{\sqrt{2bE_b}}, \quad \mathcal{B} = \frac{B_b}{2bE_b}, \quad \sigma_0 = \mathcal{N}b \cos^2 \theta \sqrt{2bE_b}, \quad \bar{\sigma}_0 = \frac{\langle J^+ \rangle}{bE_b}. \quad (50)$$

At small magnetic field,

$$\mathcal{F}_\pm = t^2 \mathcal{A}(t) + \left(\frac{t^2}{\sqrt{t^4 + 1}} \mp 1 \right) \mathcal{B}^2 + \mathcal{O}(\mathcal{B}^4), \quad (51)$$

and the conductivities become

$$\sigma_{yy}(0) = \sigma_0 \sqrt{\frac{J^2}{t^2 \mathcal{A}} + \frac{t^3}{\sqrt{\mathcal{A}}}}, \quad \sigma_{yz} = 0, \quad \mathcal{A}(t) = t^2 + \sqrt{1 + t^4}. \quad (52)$$

B.1 Drag dominated regime

For drag dominated regime, we assume that the constant J is large enough so that the J -independent result can be neglected. We study the opposite case in the following subsection.

In this case

$$\sigma_{yy} \simeq \frac{J\sigma_0}{\mathcal{F}_-} \sqrt{\mathcal{F}_+} \ , \ \sigma_{yz} = \bar{\sigma}_0 \frac{\mathcal{B}}{\mathcal{F}_-} \ . \quad (53)$$

Inverting the conductivity tensor, we can derive the resistivity formula as

$$\rho_{yy} = \frac{\sigma_0 J \sqrt{\mathcal{F}_+} \mathcal{F}_-}{\sigma_0^2 J^2 \mathcal{F}_+ + \bar{\sigma}_0^2 \mathcal{B}^2} \ , \ \rho_{yz} = \frac{\bar{\sigma}_0 \mathcal{B} \mathcal{F}_-}{\sigma_0^2 J^2 \mathcal{F}_+ + \bar{\sigma}_0^2 \mathcal{B}^2} \ , \ \cot \Theta_H = \frac{\rho_{yy}}{\rho_{yz}} = \frac{\sigma_0 J}{\bar{\sigma}_0 \mathcal{B}} \sqrt{\mathcal{F}_+} \ . \quad (54)$$

We will also calculate the rest of the related observables. The magnetoresistance is defined as

$$\frac{\Delta\rho}{\rho} \equiv \frac{\rho_{yy}(B) - \rho_{yy}(0)}{\rho_{yy}(0)} \ . \quad (55)$$

In the drag regime, it is equal to

$$\frac{\Delta\rho}{\rho} = \frac{\sqrt{\mathcal{F}_+} \mathcal{F}_-}{(\sigma_0^2 J^2 \mathcal{F}_+ + \bar{\sigma}_0^2 \mathcal{B}^2) t \sqrt{\mathcal{A}}} - 1 \simeq \left(\frac{\sigma_0^2 J^2 (3 + \frac{t^2}{\sqrt{t^4+1}}) - 2\bar{\sigma}_0^2}{2\sigma_0^2 J^2 t^2 \mathcal{A}} \right) \mathcal{B}^2 + \mathcal{O}(\mathcal{B}^4) \ . \quad (56)$$

Here we kept two terms in the denominator because they are at the same order in the drag limit.

In the weak field regime or linear field regime, which is defined as the regime with the properties, $\frac{\Delta\rho}{\rho} \sim B_b^2$ and $\rho_{yz} \sim B_b$, the magnetoresistance has the following behavior : it diverges as $1/t^2$ as $t \rightarrow 0$ and vanishes as $1/t^4$ as $t \rightarrow \infty$.

The Hall resistance is

$$R_H \equiv \frac{\rho_{yz}}{B} = \frac{\bar{\sigma}_0 \mathcal{F}_-}{\sigma_0^2 J^2 \mathcal{F}_+ + \bar{\sigma}_0^2 \mathcal{B}^2} \simeq \frac{\bar{\sigma}_0}{\sigma_0^2 J^2} + \left(\frac{\bar{\sigma}_0 (2\sigma_0^2 J^2 - \bar{\sigma}_0^2)}{\sigma_0^4 J^4 t^2 \mathcal{A}} \right) \mathcal{B}^2 + \mathcal{O}(\mathcal{B}^4) \ . \quad (57)$$

In the drag regime, we keep both terms in the denominator. Overall, this is constant due to the first term. There are small corrections with temperature dependence. In the small field regime it behaves as t^{-2} as $t \rightarrow 0$ and t^{-4} as $t \rightarrow \infty$.

We also define the Köhler ratio K , and the modified Köhler ratio \tilde{K} as

$$K = \rho_{yy}(0)^2 \frac{\rho_{yy}(B) - \rho_{yy}(0)}{\rho_{yy}(0)} = \rho_{yy}(0)(\rho_{yy}(B) - \rho_{yy}(0)) \ , \ \tilde{K} = (\cot \Theta_H)^2 \frac{\Delta\rho}{\rho} \ . \quad (58)$$

In the drag regime we obtain for the Köhler ratio

$$K \simeq \frac{t\sqrt{\mathcal{A}}}{\sigma_0 J} \frac{\Delta\rho}{\rho} + \dots \simeq \left(\frac{\sigma_0^2 J^2 (3 + \frac{t^2}{\sqrt{t^4+1}}) - 2\bar{\sigma}_0^2}{2\sigma_0^4 J^4} \right) \mathcal{B}^2 + \dots \ . \quad (59)$$

and for the modified Köhler ratio is

$$\tilde{K} \simeq \frac{\sigma_0^2 J^2}{\bar{\sigma}_0^2 \mathcal{B}^2} \mathcal{F}_+ \frac{\Delta\rho}{\rho} + \dots \simeq \frac{\sigma_0^2 J^2 (3 + \frac{t^2}{\sqrt{t^4+1}}) - 2\bar{\sigma}_0^2}{2\bar{\sigma}_0^2} + \dots \ . \quad (60)$$

For the two regimes, $t \ll 1$ and $t \gg 1$, K and \tilde{K} are both independent of t .

B.1.1 Drag dominated regime I : $\mathcal{B} \ll t^2$

Using this condition we expand the square root as

$$\sqrt{\left(1 + \frac{\mathcal{B}^2}{t^4}\right)^2 + \frac{1}{t^4}} \simeq \sqrt{1 + \frac{1}{t^4}} \left[1 + \frac{\mathcal{B}^2}{1 + t^4} + \frac{\mathcal{B}^4}{2t^4(t^4 + 1)^2} + \dots\right]. \quad (61)$$

To expand further we have to distinguish two cases

Ia: $t \ll 1$. Then we have

$$\mathcal{F}_{\pm} \simeq t^2 \mathcal{A} \mp \mathcal{B}^2 + \mathcal{O}(\mathcal{B}^4) \simeq t^2 \dots \mp \mathcal{B}^2 + \dots. \quad (62)$$

Thus

$$\rho_{yy} \simeq \frac{1}{\sigma_0 J} t \left(1 + \mathcal{O}(t^2) + \frac{3}{2} \frac{\mathcal{B}^2}{t^2} + \dots\right), \quad \rho_{yz} \simeq \frac{\bar{\sigma}_0 \mathcal{B}}{\sigma_0^2 J^2} + \dots, \quad (63)$$

$$\cot \Theta_H \simeq \frac{\sigma_0 J}{\bar{\sigma}_0 \mathcal{B}} t + \dots, \quad \frac{\Delta \rho}{\rho} \simeq \frac{3}{2} \frac{\mathcal{B}^2}{t^2} + \dots. \quad (64)$$

Ib: $t \gg 1$ and we obtain

$$\sqrt{\left(1 + \frac{\mathcal{B}^2}{t^4}\right)^2 + \frac{1}{t^4}} \simeq 1 + \frac{1}{2t^4} + \frac{\mathcal{B}^2}{t^4} + \dots, \quad (65)$$

$$\mathcal{F}_+ \simeq 2t^4 \left[1 + \frac{1}{4t^4} - \frac{\mathcal{B}^2}{2t^8} + \dots\right], \quad \mathcal{F}_- \simeq 2t^4 \left[1 + \frac{1}{4t^4} + \frac{\mathcal{B}^2}{t^4} + \dots\right]. \quad (66)$$

Then

$$\rho_{yy} \simeq \frac{\sqrt{2}}{\sigma_0 J} t^2 \left[1 + \frac{1}{8t^4} + \frac{\mathcal{B}^2}{t^4} + \dots\right], \quad \rho_{yz} \simeq \rho_{yz} \simeq \frac{\bar{\sigma}_0 \mathcal{B}}{\sigma_0^2 J^2} + \dots, \quad (67)$$

$$\cot \Theta_H \simeq \frac{\sqrt{2} \sigma_0 J}{\bar{\sigma}_0 \mathcal{B}} t^2 + \dots, \quad \frac{\Delta \rho}{\rho} \simeq \frac{\mathcal{B}^2}{t^4 + \frac{1}{8}} + \dots. \quad (68)$$

B.1.2 Drag dominated regime II : $\mathcal{B} \gg t^2$

In this case the square root is expanded as

$$\sqrt{\left(1 + \frac{\mathcal{B}^2}{t^4}\right)^2 + \frac{1}{t^4}} \simeq \sqrt{\frac{\mathcal{B}^4}{t^8} + \frac{1}{t^4}} \left[1 + \dots\right]. \quad (69)$$

Here we also distinguish two cases.

IIa: $t \ll \mathcal{B} \rightarrow \frac{\mathcal{B}^4}{t^8} \gg \frac{1}{t^4}$. Thus

$$\mathcal{F}_+ \simeq 2t^4 + \frac{t^4}{2\mathcal{B}^2} + \frac{t^8}{2\mathcal{B}^2} + \dots, \quad \mathcal{F}_- \simeq 2\mathcal{B}^2 + 2t^4 + \frac{t^4}{2\mathcal{B}^2} + \frac{t^8}{2\mathcal{B}^2} + \dots. \quad (70)$$

and

$$\rho_{yy} \simeq \frac{2\sqrt{2}\sigma_0 J t^2}{\bar{\sigma}_0^2} \left(1 + \frac{(1+9t^2)\bar{\sigma}_0^2 - 2\sigma_0^2 J^2 t^4}{8\bar{\sigma}_0^2 \mathcal{B}^2} + \dots \right), \quad \cot \Theta_H \simeq \frac{\sigma_0 J \sqrt{1+4\mathcal{B}^2}}{\bar{\sigma}_0 \sqrt{2}\mathcal{B}^2} t^2, \quad (71)$$

$$\rho_{yz} \simeq \frac{2\mathcal{B}}{\bar{\sigma}_0} + \dots, \quad \frac{\Delta\rho}{\rho} \simeq \frac{2\sqrt{2}\sigma_0^2 J^2 t^2}{\bar{\sigma}_0^2 \mathcal{A}} \left(1 + \frac{(1+9t^2)\bar{\sigma}_0^2 - 2\sigma_0^2 J^2 t^4}{8\bar{\sigma}_0^2 \mathcal{B}^2} + \dots \right) - 1. \quad (72)$$

IIb: $t \gg \mathcal{B} \rightarrow \frac{\mathcal{B}^4}{t^8} \ll \frac{1}{t^4}$. This can only happen if $\mathcal{B} \ll 1$ and this in turn implies that $t \ll 1$. We obtain

$$\mathcal{F}_{\pm} \simeq t^2 \left[1 \mp \frac{\mathcal{B}^2}{t^2} + \dots \right], \quad (73)$$

and we have

$$\rho_{yy} \simeq \frac{1}{\sigma_0 J} \left[t + \frac{3\mathcal{B}^2}{2t} + \dots \right], \quad \rho_{yz} \simeq \frac{\bar{\sigma}_0 \mathcal{B}}{\sigma_0^2 J^2} + \dots, \quad (74)$$

$$\cot \Theta_H \simeq \frac{\sigma_0 J}{\bar{\sigma}_0 \mathcal{B}} t + \dots, \quad \frac{\Delta\rho}{\rho} \simeq \frac{3\mathcal{B}^2}{2t^2} + \dots. \quad (75)$$

Note that case IIb has the same asymptotics as case Ia.

B.2 Pair creation dominated regime

In this case, the term proportional to \mathcal{N} dominates compared to the drag term and the conductivities simplify to

$$\sigma_{yy} = \frac{\sigma_0 t^2 \mathcal{F}_+^{\frac{1}{4}}}{\mathcal{F}_-^{\frac{1}{2}}}, \quad \sigma_{yz} = \bar{\sigma}_0 \frac{\mathcal{B}}{\mathcal{F}_-}, \quad \cot \Theta_H = \frac{\sigma_0 t^2}{\bar{\sigma}_0 \mathcal{B}} \mathcal{F}_+^{\frac{1}{4}} \mathcal{F}_-^{\frac{1}{2}}, \quad (76)$$

$$\mathcal{F}_{\pm} = t^4 \left[1 \mp \frac{\mathcal{B}^2}{t^4} + \sqrt{\left(1 + \frac{\mathcal{B}^2}{t^4} \right)^2 + \frac{1}{t^4}} \right]. \quad (77)$$

B.2.1 Pair creation dominated regime I : $\mathcal{B} \ll t^2$

We have two different regimes to consider.

Ia: $t \ll 1$.

$$\mathcal{F}_{\pm} \simeq t^2 + \dots, \quad \sigma_{yy} \simeq \sigma_0 t^{\frac{3}{2}} + \dots, \quad \sigma_{yz} \simeq \frac{\bar{\sigma}_0 \mathcal{B}}{t^2} + \dots, \quad \cot \Theta_H \simeq \frac{\sigma_0}{\bar{\sigma}_0 \mathcal{B}} t^{\frac{7}{2}} + \dots. \quad (78)$$

Ib: $t \gg 1$.

$$\mathcal{F}_{\pm} \simeq 2t^4 + \dots, \quad \sigma_{yy} \simeq \sigma_0 t + \dots, \quad \sigma_{yz} \simeq \frac{\bar{\sigma}_0 \mathcal{B}}{t^4} + \dots, \quad \cot \Theta_H \simeq \frac{\sigma_0}{\bar{\sigma}_0 \mathcal{B}} t^5 + \dots. \quad (79)$$

B.2.2 Pair creation dominated regime II : $\mathcal{B} \gg t^2$

We have again two different regimes to consider.

$$\text{IIa: } t \ll \mathcal{B} \quad \rightarrow \quad \frac{\mathcal{B}^4}{t^8} \gg \frac{1}{t^4}.$$

$$\mathcal{F}_+ \simeq 2t^4 + \dots, \quad \mathcal{F}_- \simeq 2\mathcal{B}^2 + \dots \quad (80)$$

$$\sigma_{yy} \simeq \frac{\sigma_0}{\mathcal{B}} t^3 + \dots, \quad \sigma_{yz} \simeq \frac{\bar{\sigma}_0}{2\mathcal{B}} + \dots, \quad \cot \Theta_H \simeq \frac{2\sigma_0}{\bar{\sigma}_0} t^3 + \dots. \quad (81)$$

$$\text{IIb: } t \gg \mathcal{B} \quad \rightarrow \quad \frac{\mathcal{B}^4}{t^8} \ll \frac{1}{t^4}.$$

This can only happen if $\mathcal{B} \ll 1$ and this in turn implies that $t \ll 1$.

$$\mathcal{F}_{\pm} \simeq t^2. \quad (82)$$

This is again as in case Ia.

B.2.3 Condition for the drag dominated regime

The condition for the drag term to dominate over the pair-creation term in the conductivity reads from (48)

$$\frac{t^4 \mathcal{F}_-}{\sqrt{\mathcal{F}_+}} \ll J^2. \quad (83)$$

We will examine this condition in the three distinct regimes. For the region **I**: $\mathcal{B} \ll t^2$, we have

$$\text{Ia: } t \ll 1 \quad \text{with} \quad t^5 \ll J^2, \quad (84)$$

$$\text{Ib: } t \gg 1 \quad \text{with} \quad \sqrt{2}t^6 \ll J^2. \quad (85)$$

For the region **II**: $\mathcal{B} \gg t^2$, we have

$$\text{IIa: } t \ll \mathcal{B} \quad \rightarrow \quad \frac{\mathcal{B}^4}{t^8} \gg \frac{1}{t^4} \quad \text{with} \quad \sqrt{2}\mathcal{B}^2 t^2 \ll J^2, \quad (86)$$

$$\text{IIb: } t \gg \mathcal{B} \quad \rightarrow \quad \frac{\mathcal{B}^4}{t^8} \ll \frac{1}{t^4} \quad \rightarrow \quad \mathcal{B} \ll 1 \quad \rightarrow \quad t \ll 1. \quad (87)$$

Therefore **IIb** implies case Ia.

References

- [1] P. W. Anderson, "*Basic notions of condensed matter physics*," Addison-Wesley, 1984.

- [2] S. Sachdev, “*Condensed matter and AdS/CFT*,” [ArXiv:1002.2947][hep-th].
- [3] J. M. Maldacena, *The large N limit of superconformal field theories and supergravity*, Adv. Theor. Math. Phys. **2**, 231 (1998) [Int. J. Theor. Phys. **38**, 1113 (1999)].
- [4] D. T. Son, *Toward an AdS/cold atoms correspondence: a geometric realization of the Schroedinger symmetry*, Phys. Rev. D **78**, 046003 (2008).
- [5] K. Balasubramanian and J. McGreevy, *Gravity duals for non-relativistic CFTs*, Phys. Rev. Lett. **101**, 061601 (2008). [ArXiv:0804.4053][hep-th].
- [6] S. Kachru, X. Liu and M. Mulligan, “*Gravity Duals of Lifshitz-like Fixed Points*,” Phys. Rev. D **78** (2008) 106005 [ArXiv:0808.1725][hep-th].
- [7] C. P. Herzog, M. Rangamani and S. F. Ross, *Heating up Galilean holography*, JHEP **0811**, 080 (2008). [ArXiv:0807.1099] [hep-th].
- [8] J. Maldacena, D. Martelli and Y. Tachikawa, “*Comments on string theory backgrounds with non-relativistic conformal symmetry*”, JHEP **0810**, 072 (2008). [ArXiv:0807.1100][hep-th].
- [9] A. Adams, K. Balasubramanian and J. McGreevy, *Hot Spacetimes for Cold Atoms*, JHEP **0811**, 059 (2008). [ArXiv:0807.1111] [hep-th].
- [10] D. Yamada, “*Thermodynamics of Black Holes in Schroedinger Space*,” Class. Quant. Grav. **26**, 075006 (2009). [ArXiv:0809.4928] [hep-th].
- [11] M. Alishahiha and O. J. Ganor, *Twisted backgrounds, pp-waves and nonlocal field theories*, JHEP **0303**, 006 (2003). [ArXiv:hep-th/0301080].
- [12] E. G. Gimon, A. Hashimoto, V. E. Hubeny, O. Lunin and M. Rangamani, *Black strings in asymptotically plane wave geometries*, JHEP **0308**, 035 (2003). [ArXiv:hep-th/0306131].
- [13] W. D. Goldberger, *AdS/CFT duality for non-relativistic field theory*, JHEP **0903**, 069 (2009). [ArXiv:0806.2867] [hep-th].
- [14] J. L. F. Barbon and C. A. Fuertes, *On the spectrum of nonrelativistic AdS/CFT*, JHEP **0809**, 030 (2008). [ArXiv:0806.3244] [hep-th].
- [15] B. S. Kim and D. Yamada, “*Properties of Schroedinger Black Holes from AdS Space*,” JHEP **1107** (2011) 120. [ArXiv:1008.3286][hep-th].

- [16] M. Ammon, C. Hoyos, A. O'Bannon and J. M. S. Wu, "*Holographic Flavor Transport in Schroedinger Spacetime*," JHEP **1006**, 012 (2010). [ArXiv:1003.5913][hep-th].
- [17] N. E. Hussey, "*Phenomenology of the normal state in-plane transport properties of high- T_c cuprates*", J. Phys.: Condens. Matter **20**, 123201 (2008).
- [18] R. A. Cooper, Y. Wang, B. Vignolle, O. J. Lipscombe, S. M. Hayden, Y. Tanabe, T. Adachi, Y. Koike, M. Nohara, H. Takagi, C. Proust, N. E. Hussey, "*Anomalous Criticality in the Electrical Resistivity of $La_{2-x}Sr_xCuO_4$* " Science **323**, 603 (2009).
- [19] A. P. Mackenzie, S. R. Julian, D. C. Sinclair and C. T. Lin, "*Normal-state magneto-transport in superconducting $Tl_2Ba_2CuO_{6+\delta}$ to millikelvin temperatures*", Phys. Rev. B **53**, 5848 (1996).
- [20] N. E. Hussey, R. A. Cooper, Xiaofeng Xu, Y. Wang, B. Vignolle and C. Proust, "*Dichotomy in the T -linear resistivity in hole-doped cuprates*", Phil. Trans. R. Soc. A. **369**, 1626 (2010).
- [21] A. W. Tyler and A. P. Mackenzie, "*Hall effect of single layer, tetragonal $Tl_2Ba_2CuO_{6+\delta}$ near optimal doping*", Physica C **282-287**, 1185 (1997).
- [22] T. R. Chien, Z. Z. Wang, and N. P. Ong, "*Effect of Zn impurities on the normal-state Hall angle in single-crystal $YBa_2Cu_{3-x}Zn_xO_{7-\delta}$* ", Phys. Rev. Lett. **67**, 2088 (1991).
- [23] H. Takagi, B. Batlogg, H. L. Kao, J. Kwo, R. J. Cava, J. J. Krajewski, and W. F. Peck, Jr., "*Systematic evolution of temperature-dependent resistivity in $La_{2-x}Sr_xCuO_4$* ", Phys. Rev. Lett. **69**, 2975 (1992).
- [24] C. Kendziora, D. Mandrus, L. Mihaly and L. Forro, "*Single-band model for the temperature-dependent Hall coefficient of high- T_c superconductors*", Phys. Rev. B **46**, 14297 (1992).
- [25] H. Y. Hwang, B. Batlogg, H. Takagi, H. L. Kao, J. Kwo, R. J. Cava, J. J. Krajewski, and W. F. Peck, Jr., "*Scaling of the temperature dependent Hall effect in $La_{2-x}Sr_xCuO_4$* ", Phys. Rev. Lett. **72**, 2636 (1994).
- [26] J. M. Harris, Y. F. Yan, P. Matl, N. P. Ong, P. W. Anderson, T. Kimura and K. Kitazawa, "*Violation of Kohler's Rule in the Normal-State Magnetoresistance of $YBa_2Cu_3O_{7-\delta}$ and $La_2Sr_xCuO_4$* ", Phys. Rev. Lett, **75**, 1391 (1995).

- [27] N. E. Hussey, J. R. Cooper, J. M. Wheatley, I. R. Fisher, A. Carrington, A. P. Mackenzie, C. T. Lin, and O. Milat, "*Angular Dependence of the c-axis Normal State Magnetoresistance in Single Crystal $Tl_2Ba_2CuO_6$* ", Phys. Rev. Lett. **76**, 122 (1996).
- [28] A. W. Tyler, Y. Ando, F.F. Balakirev, A. Passner, G. S. Boebinger, A. J. Schofield, A. P. Mackenzie, O. Laborde, "*High-field study of normal-state magnetotransport in $Tl_2Ba_2CuO_{6+\delta}$* " Phys. Rev. B **57**, R728 (1998).
- [29] S. H. Naqib, J. R. Cooper, J. L. Tallon, and C. Panagopoulos, "*Temperature dependence of electrical resistivity of high- T_c cuprates - from pseudogap to overdoped regions*", Physica C **387**, 365 (2003).
- [30] Y. Nakajima, K. Izawa, Y. Matsuda, S. Uji, T. Terashima, H. Shishido, R. Settai, Y. Onuki, and H. Kontani, "*Normal-state Hall Angle and Magnetoresistance in Quasi-2D Heavy Fermion $CeCoIn_5$ near a Quantum Critical Point*", J. Phys. Soc. Jpn., **73**, 5 (2004).
- [31] B. Fauqué, Y. Sidis, V. Hinkov, S. Pailhès, C.T. Lin, X. Chaud, Ph. Bourges, "*Magnetic order in the pseudogap phase of high- T_C superconductors*", Phys. Rev. Lett. **96**, 197001 (2006).
- [32] Yuan Li, Victor Balédent, Neven Barisic, Yongchan Cho, Benoit Fauqué, Yvan Sidis, Guichuan Yu, Xudong Zhao, Philippe Bourges, Martin Greven, "*Nature of the enigmatic pseudogap state: novel magnetic order in superconducting $HgBa_2CuO_{4+d}$* ", Nature 455, 372 (2008).
- [33] F. F. Balakirev, J. B. Betts, A. migliori, I. Tsukada, Y. Ando and G. S. Boebinger, "*Quantum Phase Transition in the Magnetic-Field-Induced Normal State of Optimum-Doped High- T_c Cuprate Superconductors at Low Temperatures*", Phys. Rev. Lett. **102**, 017004 (2009).
- [34] R. Daou, Nicolas Doiron-Leyraud, David LeBoeuf, S. Y. Li, Francis Laliberté, Olivier Cyr-Choinière, Y. J. Jo, L. Balicas, J.-Q. Yan, J.-S. Zhou, J. B. Goodenough and Louis Taillefer, "*Linear temperature dependence of resistivity and change in the Fermi surface at the pseudogap critical point of a high- T_c superconductor*", Nature Physics **5**, 31 (2009).
- [35] M. Cubrovic, J. Zaanen and K. Schalm, "*String Theory, Quantum Phase Transitions and the Emergent Fermi-Liquid*," Science **325**, 439 (2009). [ArXiv:0904.1993][hep-th].
- [36] H. Liu, J. McGreevy and D. Vegh, "*Non-Fermi liquids from holography*," [ArXiv:0903.2477][hep-th].

- [37] T. Faulkner, H. Liu, J. McGreevy and D. Vegh, “*Emergent quantum criticality, Fermi surfaces, and AdS_2* ,” [ArXiv:0907.2694][hep-th].
- [38] G. R. Stewart, *Non-Fermi-liquid behavior in d- and f-electron metals*, Rev. Mod. Phys. **73**, 797 (2001).
- [39] S. Zaum, K. Grube, R. Schäfer, E. D. Bauer, J. D. Thompson and H. v. Löhneysen, “*Towards the Identification of a Quantum Critical Line in the (p, B) Phase Diagram of $CeCoIn_5$ with Thermal-Expansion Measurements*”, Phys. Rev. Lett. **106**, 087003 (2011).
- [40] M. Edalati, R. G. Leigh and P. W. Phillips, “*Dynamically Generated Mott Gap from Holography*,” Phys. Rev. Lett. **106** (2011) 091602 [ArXiv:1010.3238][hep-th];
M. Edalati, R. G. Leigh, K. W. Lo and P. W. Phillips, “*Dynamical Gap and Cuprate-like Physics from Holography*,” Phys. Rev. D **83** (2011) 046012 [arXiv:1012.3751 [hep-th]];
D. Guarnera and J. McGreevy, “*Holographic Fermi surfaces and bulk dipole couplings*,” arXiv:1102.3908 [hep-th];
W. -J. Li and H. Zhang, “*Holographic non-relativistic fermionic fixed point and bulk dipole coupling*,” JHEP **1111** (2011) 018 [ArXiv:1110.4559][hep-th];
W. -J. Li, R. Meyer and H. Zhang, “*Holographic non-relativistic fermionic fixed point by the charged dilatonic black hole*,” [ArXiv:1111.3783][hep-th].
- [41] T. Faulkner, N. Iqbal, H. Liu, J. McGreevy and D. Vegh, “*Strange metal transport realized by gauge/gravity duality*,” Science **329**, 1043 (2010).
- [42] S. A. Hartnoll, J. Polchinski, E. Silverstein and D. Tong, “*Towards strange metallic holography*,” JHEP **1004**, 120 (2010). [ArXiv:0912.1061][hep-th].
- [43] C. Charmousis, B. Gouteraux, B. S. Kim, E. Kiritsis and R. Meyer, “*Effective Holographic Theories for low-temperature condensed matter systems*,” [ArXiv:1005.4690][hep-th].
- [44] B. H. Lee, D. W. Pang and C. Park, “*Strange Metallic Behavior in Anisotropic Background*,” JHEP **1007**, 057 (2010). [ArXiv:1006.1719][hep-th].
- [45] B. Gouteraux and E. Kiritsis, “*Generalized Holographic Quantum Criticality at Finite Density*,” JHEP **1112** (2011) 036 [ArXiv:1107.2116][hep-th].
- [46] S. S. Pal, “*Model building in AdS/CMT : DC Conductivity and Hall angle*,” [ArXiv:1011.3117][hep-th].

- [47] G. 't Hooft, “*A Planar Diagram Theory for Strong Interactions*,” Nucl. Phys. **B72** (1974) 461.
- [48] J. M. Maldacena, “*The Large N limit of superconformal field theories and supergravity*,” Adv. Theor. Math. Phys. **2** (1998) 231-252. [ArXiv:hep-th/9711200].
- [49] A. M. Polyakov, “*String theory and quark confinement*,” Nucl. Phys. Proc. Suppl. **68** (1998) 1-8. [ArXiv:hep-th/9711002].
- [50] D. Nickel, D. T. Son, “*Deconstructing holographic liquids*,” [ArXiv:1009.3094][hep-th];
I. Heemskerk, J. Polchinski, “*Holographic and Wilsonian Renormalization Groups*,” [ArXiv:1010.1264][hep-th];
T. Faulkner, H. Liu, M. Rangamani, “*Integrating out geometry: Holographic Wilsonian RG and the membrane paradigm*,” [ArXiv:1010.4036][hep-th].
- [51] J. de Boer, E. P. Verlinde and H. L. Verlinde, “*On the holographic renormalization group*,” JHEP **0008** (2000) 003 [ArXiv:hep-th/9912012].
- [52] R. Casero, E. Kiritsis, A. Paredes, “*Chiral symmetry breaking as open string tachyon condensation*,” Nucl. Phys. **B787** (2007) 98-134. [ArXiv:hep-th/0702155];
I. Iatrakis, E. Kiritsis and A. Paredes, “*An AdS/QCD model from Sen’s tachyon action*,” Phys. Rev. D **81** (2010) 115004 [ArXiv:1003.2377][hep-ph];
“*An AdS/QCD model from tachyon condensation: II*,” JHEP **1011** (2010) 123 [ArXiv:1010.1364][hep-ph].
- [53] This is not true for the Schrödinger case [16] due to the non-trivial Kalb-Ramond field present in the solution.
- [54] E. Kiritsis, “*Supergravity, D-brane probes and thermal superYang-Mills: A Comparison*,” JHEP **9910** (1999) 010. [ArXiv:hep-th/9906206].
- [55] A. Karch and A. O’Bannon, “*Metallic AdS/CFT*,” JHEP **0709**, 024 (2007). [ArXiv:0705.3870][hep-th].
- [56] A. O’Bannon, “*Hall Conductivity of Flavor Fields from AdS/CFT*,” Phys. Rev. D **76**, 086007 (2007). [ArXiv:0708.1994] [hep-th].
- [57] G. S. Boebinger, “*An Abnormal Normal State*,” Science **323**, 590 (2009).
- [58] T. Kimura, S. Miyasaka, H. Takagi, K. Tamasaku, H. Eisaki, S. Uchida, K. Kitazawa, M. Hiroi, M. Sera, and N. Kobayashi, “*In-plane and out-of-plane magnetoresistance in $La_{2-x}Sr_xCuO_4$ single crystals*” Phys. Rev. B **53**, 8733 (1996).

- [59] Y. Ando, G. S. Boebinger, A. Passner, N. L. Wang, C. Geibel, F. Steglich, I. E. Trofimov and F. F. Balakirev, "*Normal-state Hall effect and the insulating resistivity of high- T_c cuprates at low temperatures*", Phys. Rev. B **56**, R8530 (1997).
- [60] Y. Ando, Y. Kurita, S. Komiya, S. Ono, and K. Segawa, "*Evolution of the Hall Coefficient and the Peculiar Electronic Structure of the Cuprate Superconductors*", Phys. Rev. Lett. **92**, 197001 (2004).
- [61] N. P. Ong and P. W. Anderson, "*Comment on Anomalous Hall Effect in $YBa_2Cu_3O_7$* ", Phys. Rev. Lett. **78**, 977 (1997).
- [62] S. Sachdev, "*Holographic metals and the fractionalized Fermi liquid*," Phys. Rev. Lett. **105**, 151602 (2010). [ArXiv:1006.3794] [hep-th].
- [63] S. Sachdev, "*The landscape of the Hubbard model*," [ArXiv:1012.0299] [hep-th].